Toward an Empirical Theory of Pulsar Emission. IX. On the Peculiar Properties and Geometric Regularity of Lyne & Manchester's "Partial Cone" Pulsars

Dipanjan Mitra[1]
National Astronomy and Ionosphere Center, Arecibo Observatory, HC3 Box 53995, PR 00612
and

Joanna M. Rankin[2]
Sterrenkundig Instituut "Anton Pannekoek," University of Amsterdam, Science Park 904, 1098 XH Amsterdam, Netherlands

Released 2004 Xxxxx XX

ABSTRACT

Lyne & Manchester (1988) identified a group of some 50 pulsars they called "partial cones" which they found difficult to classify and interpret. They were notable for their asymmetric average profiles and asymmetric polarization position-angle (PPA) traverses, wherein the steepest gradient (SG) point fell toward one edge of the total intensity profile. Over the last two decades, this population of pulsars has raised cautions vis-a-vis the core/cone model of the radio pulsar emission beam which implies a high degree of order and symmetry. In this paper we investigate new single pulse polarimetric observations of 39 of these "partial cone" pulsars, observed with the Giant Meterwave Radio Telescope in India and the Arecibo Observatory in Puerto Rico. These highly sensitive single pulse observations help us to establish that the "partial cones" generally exhibit a core/cone structure just as "normal" pulsars do. Further, we find that aberration-retardation effects play a significant role in distorting the core/cone structure of the radio emission beam in rapidly rotating pulsars. We also find several additional examples of highly polarized pre- and postcursor features that appear to be generated at high altitude, far from the usual polar flux-tube emission sites of the core and conal radiation.

Subject headings: miscellaneous – methods:MHD — plasmas — data analysis — pulsars: general, individual — radiation mechanism: nonthermal – polarization

I. Introduction

The term "partial cones" was introduced in Lyne & Manchester's (hereafter L&M) well known 1988 radio-pulsar beamform study to describe a group of profiles that were not easily classified as falling into one of their cone- or core-dominated categories. They confirmed that the majority of their 200 or so pulsars showed a highly ordered, roughly symmetric, quantitatively consistent beam geometry. By contrast, their largish residuum of pulsars with unclassifiable, asymmetric profiles were dubbed "partial cones", because a number (*e.g.*, B0540+23) had asymmetric profiles reminiscent of one side of a classic conal double profile (*e.g.*, B0525+21). This group of unclassifiable pulsars raised strong cautions—indeed, if some 20-30% of profiles cannot be classified in terms of cores and cones, is this model not itself

[1]National Centre for Radio Astrophysics, Ganeshkhind, Pune 411 007 India: dmitra@ncra.tifr.res.in

[2]Physics Department, 82 University Place, University of Vermont, Burlington, VT 05405 USA: Joanna.Rankin@uvm.edu

suspect? Given these patently inscrutable profiles, often with puzzling asymmetries, they left open the possibility that a "patchy" pattern of components resulted from "hot spots" on the polar cap.

The major purpose and overall theme of this "Empirical Theory" series has been demonstrating the geometric orderliness of most pulsar emission. Species of profiles were defined in Paper I (*e.g.*, Rankin 1983a; see the References for further series numbers). Their commonalities in terms of spectral behavior and modulation were studied in Papers II and III. The geometric regularities of core components in relation to the polar cap was introduced in Paper IV. Paper VI then presented a comprehensive analysis of quantitative pulsar emission geometry using the core-cone model. And three other numbers (Papers V, VII and VIII) have respectively discussed circular polarization, radio-to-frequency mapping, and edge depolarization. The results of Paper VI were sufficiently surprising that several groups carried out critical studies or independent analyses (Bhattacharya & van den Heuvel 1991, Gil *et al* 1993; Kramer *et al* 1994; Mitra & Deshpande 1999), and the core/double cone model of pulsar emission profiles was fully vetted. We thus reemphasize that L&M's work and ours provide highly compatible geometrical results for a majority of pulsars in our largely common population, so the differing interpretations of the two analyses turn importantly on L&M's group of "partial cone" pulsars.

No further systematic study of L&M's "partial cones" has been carried out over the last two decades, so this group of some 60 pulsars remains in many workers minds as strong evidence for unsystematic pulsar beaming and perhaps polar-cap "hot spots". L&M's study was based solely on average profiles; now however, not only are much more sensitive observations often available, but pulse-sequence (hereafter PS) polarimetry has been carried out for a large fraction of these "partial cones". Surely we concur that many of the "partial cones" present particular difficulties of interpretation. We now know that L&M were partially correct in their "partial cone" moniker, as some pulsars do illuminate their polar caps very asymmetrically or episodically (Rankin *et al* 2006a)—producing lopsided or distorted profiles—but when studied closely these also exhibit orderly profile dimensions in relation to the polar cap.

A further set of pulsars with conal single profiles, we now know from detailed studies, very often exhibit highly asymmetric profiles (*e.g.*, B0943+10; Deshpande & Rankin 2001) despite strong evidence that their emission cones are produced by subbeam carousels rotating through our sightline. Aberration/retardation (hereafter A/R) effects have been identified in a number of slower pulsars (*e.g.*, Blaskiewicz *et al* 1991), and clearly may have strong effects in faster pulsars. Also, recent researches have revealed highly polarized profile features—*e.g.*, the "precursors" in pulsars B0943+10 and B1822–09 (see Backus *et al* 2010)—and even the entire profiles of particular stars (*e.g.*, B0656+14, Weltevrede *et al* 2006a) that exhibit such dissonant properties that we are forced to question whether some new non-core/cone emission process is entailed!

Generally the average profile of a radio pulsar has a characteristic steep outer edge, which apparently reflects the emitting region along the boundary of the "open" magnetosphere (or polar flux tube) adjacent to the closed field region. Beamed emission in pulsars also can explain the high linearly polarized power observed in pulsars, where the fractional linear can be as high as 70-80%. For a large number of pulsars the polarization-position angle (PPA) across the pulse profile is seen to execute a smooth 'S-shaped' curve, which according to the rotating-vector model (RVM) proposed by Radhakrishnan & Cook (1969) is taken as evidence for emission arising within the polar flux tube and centered around the magnetic axis. Within the RVM the steepest-gradient (hereafter SG) point (or the point of inflexion) of the 'S-shaped' curve is interpreted as the plane containing the magnetic dipole axis, and is often located towards the center of the profile.

Most profiles, however, tend to be asymmetric with the central core component of triple or five-component forms seen to lag the centers of their conal-component pairs. Studies by Malov & Suleimanova (1998), Gangadhara & Gupta (2001), Gupta & Gangadhara (2003), Mitra & Li (1999), and Dyks *et al* (2004) demonstrate that aberration/retardation (hereafter A/R) effects arising due to emission from a finite height within the pulsar magnetosphere can give rise to the observed profile assymetries. Once this A/R effect is properly taken into account, the emission can be understood as nested conal emission.

"Partial cones" however, are difficult to explain within the conal beam model. L&M suggested that partial cones are perhaps pulsars where only part of the polar cap is illuminated—and hence any pulsar emission-beam model should be able to reproduce partial cones. This line of argument certainly gives edge to the patchy beam model of L&M. More recently Karasterigiou & Johnston (2007) proposed a synergy between the patchy and conal beam model, where the conal emission ring is illuminated in patches.

Partial cones were identified by L&M as pulsars with profiles having one steeply rising edge and another slowly falling edge. Or, as stars where the steepest gradient point of the PPA traverse is located towards one edge of the profile. Identification of partial cones thus requires unambiguous determination of the SG point of the PPA swing with respect to its total intensity profile. It is often difficult to discern the character of the PPA traverse using only average-profile polarimetry, as did L&M. This is particularly so due to the presence of the "orthogonal" polarization modes (hereafter OPMs), which indeed are not always orthogonal (*e.g.*, Ramachandran *et al* 2004). Departures from modal orthogonality tend to produce complex average PPA behaviours, because their relative power often varies strongly with pulse longitude, and these can in turn lead to serious misinterpretations of a pulsar's PPA traverse. Hence, polarimetry of individual pulses is necessary to distinguish the OPMs and correctly assess the geometrical bases of the PPA swings (*e.g.*, Gil & Lyne 1995).

We then proceed as follows: §II describes our GMRT and Arecibo observations, and in §III we discuss our analyses of those pulsars exhibiting "flared" or episodic emission. §IV presents the large subset of "partial cone" pulsars with narrow conal profiles. In §V we introduce new analyses of pulsars with clear signatures of A/R in their emission, and in §VI we discuss the several stars with apparently aberrant polarization—components with nearly complete linear and flat PPA traverses. §VII then presents our overall geometrical analyses, and §VIII gives a summary and discussion of our results. The Appendix then discusses the properties of L&M's "partial cone" population individually.

II. Observations and Data Analysis

Our observations encompass of 39 of the 50 pulsars identified as "partial-cone" or likely "partial-cone" objects by L&M (their tables 4 & 5). We have observed these pulsars using the Giant Meterwave Radio Telescope (GMRT) at 325 MHz (P band) and the Arecibo (AO) instrument at P and/or L (1100-1700 MHz) band in full polarization.

The GMRT (Swarup *et al* 1991) is an array of 30 45-m antennas, spread over a 25-km region 80 km north of Pune, India. It is primarily an aperture-synthesis interferometer but can also be used in a phased-array configuration. The GMRT operates at multiple frequencies (150, 235, 325, 610 and 1000 - 1450 MHz) and has a maximum bandwidth of 32 MHz, split into upper and lower sidebands of 16 MHz each. At 325 MHz, which is the frequency of interest here, the feeds are linearly polarized and converted to circulars using a hybrid. Our observations were carried out on 14 February 2006 and 26 October 2007 using the phased-array mode (Sirothia 2000; Gupta *et al* 2000), in which the voltage signals of the upper sidebands from each antenna were first added coherently and then fed to the pulsar receiver. The pulsar backends computed the auto- and cross-polarized power between the two circularly polarized signals, and these were finally recorded with a sampling time of 0.512 msec. A suitable calibration procedure as described in Mitra *et al* (2005) was applied to the observations to recover the calibrated Stokes parameters I, Q, U and V. The AO observations were carried out at both 327 and 1400 MHz in a manner very like that reported in Rankin *et al* (2006a).

The calibrated Stokes parameters were used to compute the total linear polarization $L(=\sqrt{U^2+Q^2})$ and the PPA $\chi(=0.5\tan^{-1}(U/Q))$ of the several pulse sequences (hereafter PSs). Table A1 gives the various observational parameters for "partial-cone" pulsars. Table A2 then reviews some of the properties of these "partial cone" pulsars. In a number of cases we have fitted the RVM to the PPA traverses using the Everett & Weisberg (2001) convention, and these results are used in the geometric analyses that are summarized in Table A3 and discussed below.

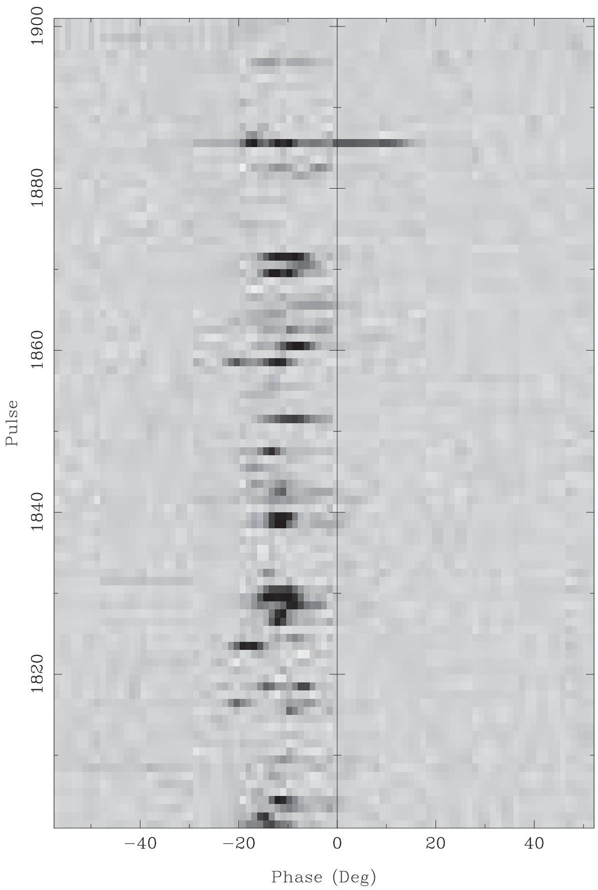

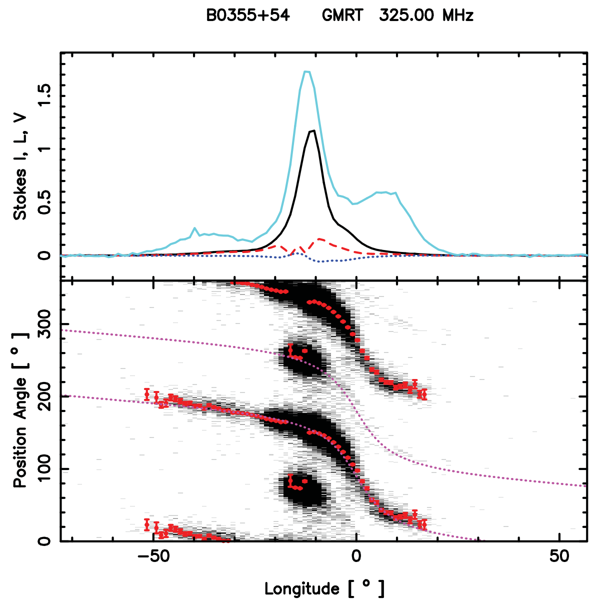

Fig. 1.— **LEFT:** Individual pulse display showing a 100-pulse sequence (1800–1900) of B0355+54. The longitude origin corresponds to the SG point of the PPA swing. Notice the sudden flaring that occurs at pulse 1886. **RIGHT:** Hybrid polarization and "flared"-emission plot for B0355+54. The bottom panel gives the PPA histogram along with the fitted RVM curve (shown twice for clarity). The top panel shows the average-profile polarization (black: total power; red: linear; blue: LH-RH circular), while the cyan curve shows the "flared" profile (see text).

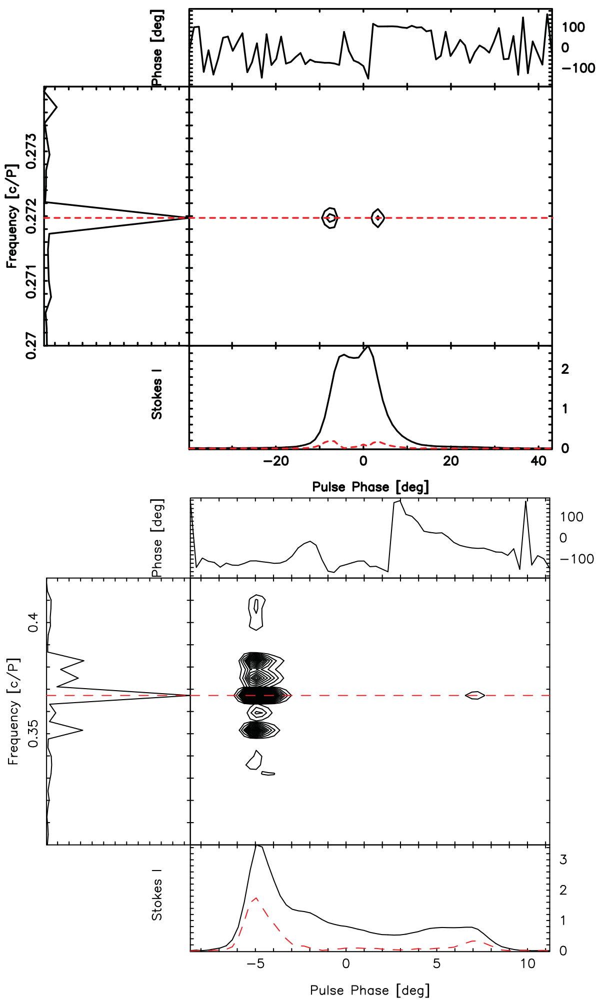

Fig. 2.— Fluctuation spectra for pulsars B0740–28 and B1910+20. The main panels show the fluctuation amplitudes in contours, and the longitude-averaged aggregates are given in the lefthand panels. The bottom panels show the total-power average profiles, and the fluctuation phases are given in the top panels.

III. "Flared" emission

Single pulses of pulsars show a great deal of variety. Generally, subpulses of varying intensity are seen to appear and disapper at various pulse longitudes, but when averaged together a stable pulse profile is formed. However, this is not always so: a few pulsars are known for their "giant" pulses—most famously the Crab pulsar—and in a few others occasional bright pulses can be so very strong that the profile form is unstable (*e.g.*, B0656+14; see Weltevrede *et al* 2006b). For a few other pulsars, "episodic" illumination has been observed that greatly emphasizes parts of a pulsar's profile at the expense of others (Rankin *et al* 2006a). For these reasons we thought it important to explore whether these effects could be active in some of L&M's "partial cone" pulsars. Almost immediately, we discovered "flaring" effects in the single pulse emission of some of these pulsars.

In the lefthand panel of Figure 1 we show a GMRT total-power pulse sequence (hereafter PS) of the "partial cone" pulsar B0355+54 (pulse #s 1800-1900). Notice that most of the bright emission occurs around $-10°$ longitude (where zero longitude corresponds to the SG point of the PPA traverse); however, one strong subpulse can be seen extending to $+15°$ (pulse #1886) and several other fainter subpulses can be discerned around $-40°$. Obviously, this pulsar shows great dynamicity in its pulse-to-pulse f luctuations: the core varies dramatically in intensity, often disappearing entirely; the leading and trailing conal outriding components are only occasionally detectable; and overall the pulsar nulls for some 30% of the time. These occasional "flares" of the conal components are then remarkable—and we find that they are very rare in B0355+54—occurring in only 200 pulses in a PS of 13000 individual pulses.

We have searched for "flared" emission in the entire set of "partial cone" pulsars available to us. We used a "tunable" window to detect sporadic emission in the fainter regions of the average profile where the intensity is close to the noise level. Each time the emission exceeded three times the noise level (averaged over the window), we marked that pulse and window as having "flared" and with adjacent windows computed the average "flared" profile. We then repeated this process for different window sizes until the "flared" profile was stable over a ranges of window widths. The righthand display of Fig. 1 gives an example of this "flared"-profile analysis for B0355+54; the upper panel shows the usual average polarized profile information (Stokes I, L and V are given by solid black, dashed-red and dotted-blue curves, respectively), and the "flared" total power profile is shown using a solid cyan curve. Obviously, this "flared" profile shows the contributions of the sporadic emission to the far edges of the profile, and it strongly suggests a three-component structure.

We found evidence for "flaring" in about half the group of "partial cone" pulsars under study, and the full results are shown using displays similar to Fig. 1 in the Appendix. Overall, we found little difference between the widths of the "flared" profiles compared to the full discernible widths of the corresponding normal average profile; however, the structure was often more scrutable—and in some cases we used these "flared" widths in the geometric analyses given in Table A3; see the Appendix for discussions of the analyses of the individual pulsars. We also looked for periodicities in the "flares" and found no evidence for any regular repetitive behavior.

IV. Conal Profile Asymmetry and Symmetry

Conal single pulsar B0809+74 was listed by L&M as a partial cone because of the strong evidence that its meter-wavelength profiles are asymmetric because they are incomplete—or "absorbed" (*e.g.*, see Rankin *et al* 2006b), and we now know that a number of other conal single pulsars share this asymmetric property (*e.g.*, B0943+10, see Deshpande & Rankin 2001). Perhaps the asymmetry is due to the circumstance that stars with such profiles entail a highly tangential sightline traverse along the outer edges of their conal beams—but although we do not understand the cause of these asymmetries adequately, we do now know that nearly all conal single ($\mathbf{S}_d$) profiles—and many narrow inner-cone double (**D**) profiles—are asymmetric.

Perhaps then unsurprisingly, we found that a large proportion of the "partial cone" pulsars identified by L&M had conal profiles that were either single ($\mathbf{S}_d$) or unresolved double (**D**) profiles. Many or most such pulsars exhibit regular drifting subpulses and consequently show features indicative of periodic modulation in their fluctuation spectra. We computed fluctuation spectra similar to those in Figure 2 for each of the PSs available to us (most are not shown), and we also consulted the published fluctuation-spectral compendia of Weltevrede *et al* (2006b, 2007; hereafter WES/WSE). Those dozen or so "partial cone" pulsars found to have $\mathbf{S}_d$ or **D** profiles—in a number of cases it was difficult to be sure which—are so denoted in Table A3, and their full analysis is discussed in the Appendix.

For a few other pulsars in our sample we found subpulse modulation features on both the leading and trailing edges of their profiles. Fig. 2 shows fluctuation spectra for pulsars B0740–28 and PSR B1910+20, where same periodicity modulates both edges of their profiles in a stationare manner. If their subpulse "drift" is produced a carousel-beam system rotating about the magnetic axis, then this strongly indicates that the emission from these stars does indeed fill most of their polar flux-tube regions.

IV. The SG point and Profile Symmetry

We have revisited these symmetry issues for all these pulsars for which we have high quality single pulse polarimetry. Our intent has been to determine whether the SG point of the PPA traverse, determined using RVM fitting, leads or lags the total intensity profile center. PPA polarimetry often helps to identify regions of OPM activity which otherwise can complicate the average-PPA traverse, and hence cause an inaccurate identification of the SG point. Thus, we have computed PPA histograms for each of the "partial cone" pulsars—which are reproduced in the Appendix—and wherever possible distinguished their separate PPA traverses before fitting the RVM to determine the SG point. In a few cases PS polarimetry was unnecessary to fix the SG point; however for pulsars like B1604–00, B2043–04 or B2217+47, mode separation was essential before any sensible RVM fit could be made to their PPA traverses.

For several other pulsars, B1910+20 and B2327–20 among them, the average PPA traverse exhibited highly non-RVM behavior. Mitra *et al* (2007) noticed for pulsar B0329+54 that the PPA traverse can be intensity dependent, and we

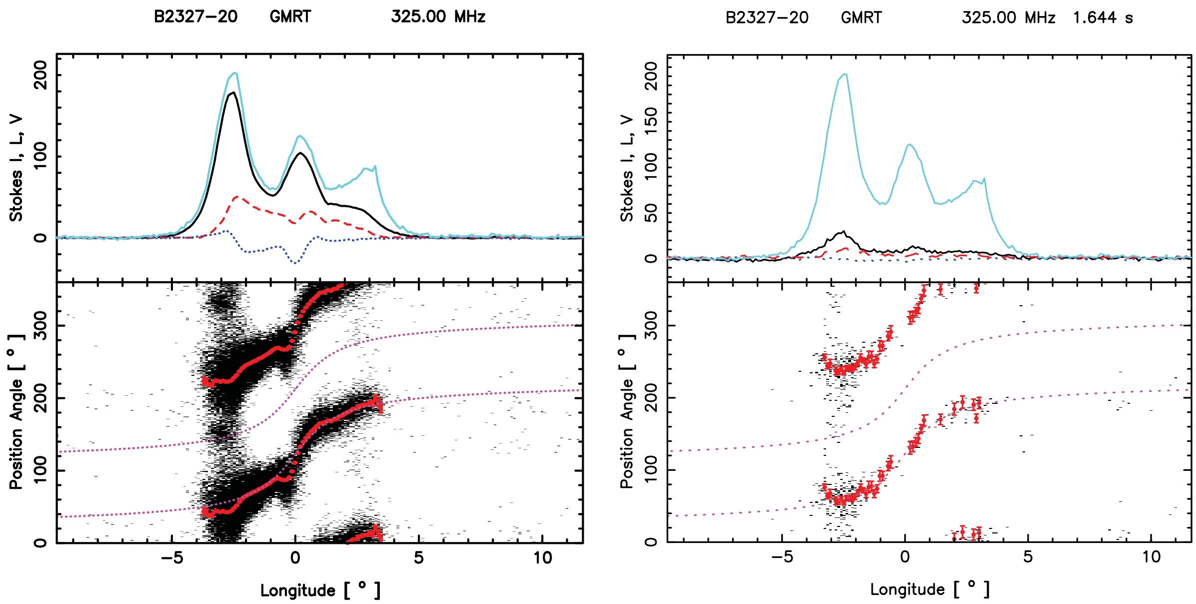

Fig. 3.— PPA histograms for pulsar B2327–20 as in Fig. 1 (right panel). The lefthand display shows the full PS, whereas the righthand plot includes only pulses having a lower intensity level. Notice that the latter PPA traverse is much smoother and can be used to fit the RVM. The longitude origin corresponds to the SG point of the PPA swing.

have used their technique of dividing the PS into intensity fractions in order to obtain a smooth PPA traverse. Figure 3 shows for pulsar B2327–20 how an apparently orderly RVM behavior can be recovered for fitting even when the total PPA profile is distorted by intensity effects. Here, the SG point obtained by fitting the RVM is well constrained. However, several pulsars in our sample (such as B0809+74 and B1112+50) show relatively flat PPA traverses, and hence the SG point is not well constrained. Given all these various circumstances, we were able to obtain RVM fits for 26 pulsars, wherein we believe that the SG points are reliable for 23 of them. The details of the fits for the individual objects are described in the Appendix, and of course we must bear in mind that all these RVM fits entail very large correlations ($\gtrsim 98\%$) between the resulting values of α and β (see Everett & Weisberg 2001).

Of primary importance is the location of the SG point with respect to the overall extent of at pulsar's profile, so as to access whether A/R is significant. We use the BCW method of finding the profile center—*i.e.*, measuring the midway point between the outer 10%-intensity points of the profile, and we then compare this with the location of the SG point. Out of the 23 pulsars with robust SG points determined, we find that for 19 the SG point trails the midway point. In two cases, B0138+59 and B2224+65, does the SG point fall convincingly towards the leading part of the profile, and for two more cases B2043-04 and B2327-20 the SG point is consistent with being coincident with the profile center. For the remaining stars the SG point is not well determined. The rightmost column of Table A2 gives an overview of these SG-point locations with respect the respective profile midpoints; here "L" refers to the case where the SG point leads the midway point, "T" where SG point is trails, "U" refers to unclear cases where the midway or the SG point determination fails and "–" refers to the cases where the profile center is consistent with being coincident with the SG point.

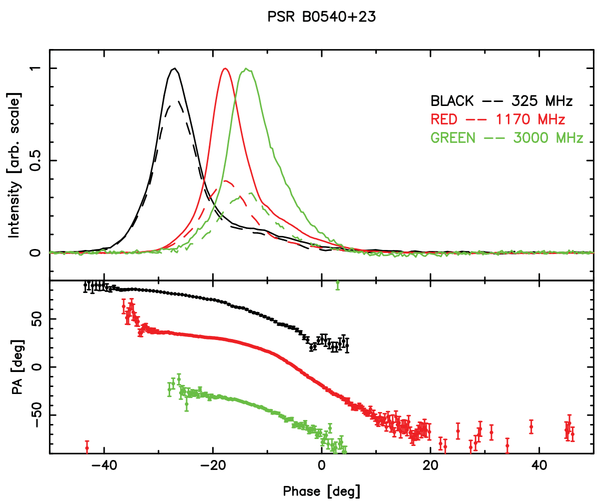

Fig. 4.— Polarized profiles for pulsar B0540+23 aligned relative to their respective SG points (327 MHz, black; 1170 MHz, red from Arecibo Observatory and 3100 MHz, green from Parkes radio telescope, Johnston et al. 2008). In each case, the RVM-fitted SG point falls at the longitude origin. The respective PPA values have been displaced vertically by arbitrary amounts for clarity. This effect must certainly be a result of A/R.

V. Abberation/Retardation Effects

We saw just above that the PPA-traverse SG points trail the profile centers in the great majority of cases. A natural explanation for this circumstance is the abberation/retardation (A/R) effects first studied by Blaskeiwicz *et al* (1991; BCW). This BCW model provided a substantial improvement over the RVM model, by incorporating these (A/R) relativistic effects on pulsar-emission properties. For emission arising from a finite height r_{em} above the center of a rotating neutron star with period P_1, they derived an expression for the PPA χ as a function of pulse longitude φ as,

$$\chi = \tan^{-1}\left(\frac{\sin\alpha\sin(\varphi-\varphi_\circ) - 3\hat{r}\sin\xi}{\sin\xi\cos\alpha + \cos\xi\sin\alpha\cos(\varphi-\varphi_\circ)}\right) + \chi_\circ \quad (1)$$

where $\hat{r}$=r_{em}/r_c is the emission height r_{em} in terms of the light-dylinder radius r_c=$cP/2\pi$. Here, the angle $\xi = \alpha+\beta$, where α is the magnetic latitude, β is the sightline impact angle, $\chi_\circ$ and $\varphi_\circ$ are arbitrary PPA and longitude offsets, and c is the speed of light. Note that eq. 1 reduces to the RVM for r_{em} tending to zero.

In short, the BCW model predicts that for radio emission arising from a constant finite height, the overall PPA traverse will lag the total intensity profile. To first order, particularly for slowly rotating pulsars, this shift is a simple translation of the PPA traverse towards the trailing parts of the profile—hence no change is required to fit the RVM to the PPA traverse. However, the SG point will now be found to lag the profile center by an amount $\Delta\varphi$= $4\pi r_{em}/Pc$, a shift which has been observed in several pulsars (*e.g.*, BCW, von Hoensbroech & Xilouris 1997, Mitra & Li 2004) and then used to estimate the relevant radio emission heights—giving typical values of a few hundred kilometers.

Here we want to justify our conclusion that for the majority of "partial cone" pulsars, the lagging of the SG point with respect to the profile center is primarily due to A/R effects. On the one hand, the "flared" profile analysis provides a valuable method of assessing the full emission width in longitude—that is, the total extent of emission activity within the polar flux-tube region—and this in turn permits us to be more certain about the position of a profile's center and thus the relative placement of the SG point. Then, on the other hand, the RVM fitting often permits us to be sure about the symmetry properties of the PPA traverse and thus its placement relative to the profile center. The shift $\Delta\varphi$ is hence found as the difference between the (conal component-pair) profile center and the SG point, and it is from this quantity that an emission height can be computed.

Among our "partial cone" population, we found 14 cases for which an A/R emission height could be computed as above, and these are tabulated in Table A4. Note that the values obtained are roughly 300-400 km—therefore not very different from those height estimates computed for normal (non-"partial cone") pulsars. This result strongly supports the conclusion that majority of the "partial cone" pulsars are very similar to other "normal" pulsars—that is, their emission arises from similar heights and (at least sometimes) involves most of the polar cap region. For the few slower pulsars in the "partial cone" population, PSR B1910+20, B2043–04 and B2327–20, the measured A/R shifts are small, such that the profile center and SG point are almost coincident. This leads to difficulty in measuring the A/R shifts (seen as negative shift values in Table A4 (see also a detailed discussion by Mitra & Li (2004) on factors affecting A/R-shift measurements).

In certain cases, the A/R effect appears quite dramatic and may well produce such large shifts that a profile form may be distorted so much that it is not easily viewed in core/cone terms. One such example is B0540+23, and in Figure 4 we overlay the polarization profiles at three frequencies and align them according to their respective SG points (at the longitude origin). The displacement of the lower frequency profiles—that evidently are emitted at ever larger heights—is many degrees of longitude for this 246-ms star. Note the triangular "tail" of emission in the 327-MHz profile that is missing or much less prominent in the other two profiles at higher frequencies. Were this 327-MHz emission emitted over a range of heights with progressively increasing A/R shifts, then the low frequency profile structure could be explained naturally. (On the other hand, it is possible that the trailing part of the profile is indeed rather weak, implying that the emission peak is leading conal emission.) While this is the most insightful example of such effects in our "partial cone" population, we note that similar effects have been found by Karastergiou & Johnston (2006) in B1054–62 and B1356–60, the latter of which is discussed below in the Appendix with the other "partial cones". Several other cases where A/R appears to affect the profile structure are denoted by "ar" in their Table A3 classifications.

VI. Aberrant Linear Polarization Signatures?

Our recent analyses (Backus *et al* 2010) on the precursor components of pulsars B0943+10 and B1822–09, strongly suggest that these features are "other"—that is, they are not emitted at low altitude in the polar flux tube as is the conal and core emission with which we are familiar. We argued that the precursors were aberrant largely on the basis of their nearly complete linear polarization and flat PPA traverses. Among L&M's "partial cone" grouping, we encounter B1822–09 again, and the geometric analysis in Table A3 (see also Fig. A6) reflects the conclusions of the above study in that we do not regard the star's precursor component as a part of its main pulse.

Three other such objects were found among L&M's "partial cones", B1322+83, B1530+27 and B2224+65. In the first case seen in Fig. A3, the highly polarized feature is a precursor to what otherwise is probably a conal single main pulse; whereas, for the latter two in Fig. A3 and A10 the aberrant feature falls as a postcursor to what seems to be a conal single and core-single main pulse respectively. A number of other such features can now been found in the published polarimetry, but at the time of L&M's study, very few were known, so it is not surprising that they regarded them as outstanding in core/core terms. Indeed, they yet remain so, but we now know of enough that they represent something a distinct phenomenon.

For B1322+83, we note also that were this star an asymmetric conal double (which is not what we conclude), the putative profile midpoint at about $-4°$ falls far ahead of the SG point under the trailing feature. Following this interpretation we can compute an A/R emission height for some 3700 km, which is very large for any pulsar. Therefore this interpretation is almost certainly incorrect.

VII. Analyses of the Emission Geometry

Paper VI of this series gave an extensive analysis if the emission geometry of some 200 pulsars. The core-component width was often used to estimate the magnetic latitude α; the sightline impact angle β was then fixed using α and the PPA sweep rate $\Delta\chi/\Delta\varphi$; and the conal radii were computed using the dimensions of the conal components or pairs. Several of the "partial cone" pulsars under study here were also studied in this analysis, but the results—based entirely on average-profile dimensions—were disappointing—just as they were for L&M and for virtually the same reasons.

Here we are now in a position to reinvestigate the emission geometry of L&M's "partial cone" population with much more information and thus a greatly enhanced expectation of success. The pulsar-by-pulsar discussions in the Appendix summarize the RVM-fitting results for all those stars for which it was possible, and Table A3 gives the PPA sweep rate R in boldface when determined by this fitting. Similarly, this table shows α in boldface when it was possible to estimate it from a core width or by other means. Then, the conal dimensions are computed from the profile width information just as was done previously in Paper VI. The outside half-power widths of the respective inner and outer conal beams are given along with the estimated emission heights—and the parameter β/ρ is also tabulated for many pulsars as an indication of the expected profile form.

These geometric results are then plotted in Figure 5, and the results are quite dramatic. The values fall on two parallel tracks representing the outer and inner conal radii, respectively. The solid symbols indicate the full solutions above, and the open ones compatibility where α could not be determined independently. Overall we see that there is no geometric distinction at all between L&M's "partial cone" pulsars and those with more ordinary and symmetrical profiles. Of course, all of the "partial cone" pulsars for which we have observations are not represented in Fig. 5—some of them are very difficult to understand as we have seen in the previous section—but here we see clearly that the great majority exhibit the same orderly conal and core dimensions as was found earlier in Paper VI.

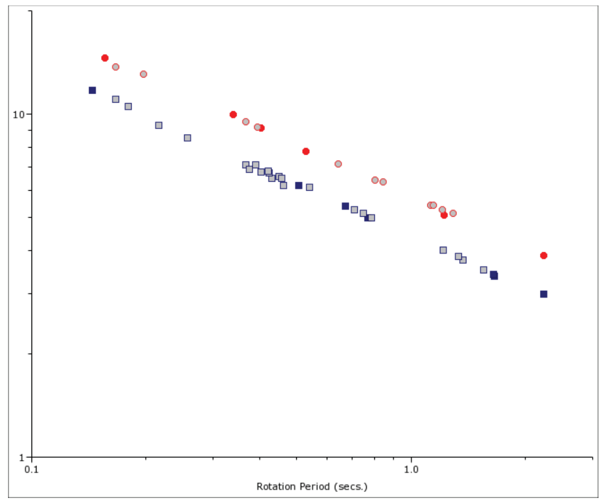

Fig. 5.— Plot showing (outside half-power) conal emission radius ρ vs. rotation period P_1 for the "partial cone" population of pulsars in Table A3. The red symbols represent the outer cones and the blue the inner cones, respectively. The filled symbols reflect a full analysis where the magnetic latitude α can be determined and β then determined from the fitted PPA sweep rate R; whereas the open symbols show the compatibility of other pulsars when α cannot be independently estimated.

VIII. Summary and Conclusion

In the foregoing sections we restudied the population of "partial cone" pulsars so identified by Lyne & Manchester in 1988. Using a combination of recent GMRT and Arecibo polarimetry, we have based our analyses predominantly on sensitive PS observations. These analyses have attempted to identify regions of "flared" and A/Red emission as well as searching for the more usual periodic subpulses modulation.

Through this analysis we have been able to show that—

- In general, the L&M's "partial cone" pulsars exhibit no particular property or difference as compared to the rest of the slow pulsar population. Rather, they exhibit a range of characteristics, many of which are well understood and some of which are not.

- Overall the "partial cones" exhibit cone and double cone profile structures just as the "normal" pulsars do. To a significant extent PS analyses are needed to establish this regularity, because many of the "partial cones" do preferentially illuminate only a part of their polar flux-tube emission regions. However, when these small difficulties are accounted for, the emission geometry of most "partial cones" is remarkably regular in the terms established in Paper VI—that is, both the cores and cones have particular angular dimensions that scale with the size of a pulsar's polar cap.

- We find several further examples among the "partial cones" of highly polarized pre- or postcursors with flat PPA traverses. Following our analysis of such features in B0943+10 and B1822–09, we argued that these features cannot be emitted at low altitude within the usual polar flux-tube region. Such features are important, because they provide clues to the electrodynamics of the larger magnetosphere. Clearly this emission is coherent (highly polarized), beamed and likely emitted at very high altitude.

- A number of examples of A/R shifts, both in the PPA traverses and component positions, were encountered among the "partial cones". It seems likely that A/R is an important factor in distorting the core/cone structure of pulsars that rotate quite rapidly.

Lyne & Manchester in 1988 did not, of course, regard A/R as a strong factor in the structure of pulse profiles. This led them to conclude that in certain pulsars parts of the conal emission is missing. Our detailed analysis of this "partial cone" group reveals that, for most, the SG point trails the profile center—which is in itself a strong indication of A/R effects. The other effect that A/R predicts—that the intensity of the leading conal regions of the profile will be brighter than the trailing parts—this we do not see in our analyses. Rather it appears that the probability of radio emission across the pulse profile (or within the polar flux tube) varies strongly. For example, the "flared" emission we see in several stars (*e.g.*, PSR B0355+54 in Fig 1) is overall rare, occurring within only 1-5% of all active pulse longitudes, whereas in many other such regions the emission is virtually continuous, occurring essentially 100% of the time. Of course, this implies that the shape of a pulsar's total-intensity profile varies strongly across the "active" window because several different processes entailed in this emission also vary strong with longitude. The PPA traverse, on the other hand, closely follows the RVM (particularly when complications due to OPM and A/R effects can be accounted for).

Hence, the phenomenological model that emerges from our overall analyses is that pulsar coherent radio emission almost always arises from open dipolar field lines, at several hundred km above the pulsar polar cap. Within this polar flux-tube region, there is an underlying double cone/core structure of the pulsar radio-emission beams, although the pulse shape itself depends on the probability of coherent radio emission (P_{cre}), which varies strongly with magnetic colatitude and azimuth and thus with pulse longitude along the sightline trajectory of a given star and viewing geometry. For example, under the vaccum-gap model and assuming curvature radiation as the radio emission mechanism, P_{cre} should be viewed as a combined probability of $P_{cre} = P_{ppc} \times P_{spc} \times P_{ccr}$. Here P_{ppc} is the probability of primary pair creation in the vaccum gap, P_{spc} is the probability of secondary pair creation and P_{ccr} would be the criteria for exciting coherent curvature radiation

(RS75, Sturrock 1971, Gil, Lyubarsky & Melikidze 2004). Further since average pulse profiles are stable, P_{cre} fluctuates around a mean value, indicating the presence of a stable physical quantity at every pulse longitude. We conjecture that P_{cre} is primarily guided by the underlying multipolar magnetic field across the polar cap. Such a structure causes the field to vary in magnitude and curvature radius across the polar cap (see Gil, Melikidze & Mitra 2002). The field at the region where radio emission arises is however significantly dipolar.

We are pleased to acknowledge S. Sarala for important assistance with aspects of the observations and analysis of GMRT data. We thank our first referee Aris Karastergiou for encouraging us to enlarge our study to include as many of L&M's "partial-cone" pulsars as possible. We thank the staff of the GMRT that made these observations possible. We also wish to thank Joel Weisberg for his assistance with the ionospheric Faraday rotation corrections. One of us (JMR) thanks the Anton Pannekoek Astronomical Institute of the University of Amsterdam for their generous hospitality and both Netherlands National Science Foundation and ASTRON for their Visitor Grants. Portions of this work were carried out with support from US National Science Foundation Grants AST 99-87654 and 08-07691. Arecibo Observatory is operated by Cornell University under contract to the US NSF. GMRT is run by the National Centre for Radio Astrophysics of the Tata Institute of Fundamental Research. This work used the NASA ADS system.

REFERENCES

Backus I., Mitra, D., & Rankin, J. M., 2010, M.N.R.A.S., in press.

Bartel, N., Kardeshev, N. S., Kuzmin, A D., Nikolaev, N.Ya., Popov, M.V., Sieber, W., Smirnova, T.V., Soglasnov, V.A., & Wielebinski, R. 1981, A&A, 93, 85.

Bartel, N. 1981, A&A, 97, 384.

Bhattacharya, D. & van den Heuvel, E.P.J. 1991, Physics Reports, 203, 1-124

Biggs, J. D., 1990, M.N.R.A.S., 246, 341.

Blaskiewcz, M., Cordes, J.M., & Wassermann, I. 1991 Ap.J., 370 643 (BCW)

Costa, M. E., McCulloch, P. M., & Hamilton, P. A. 1991, M.N.R.A.S., 252, 13 (CMH)

Deshpande, A. A. & Rankin, J., 2001, M.N.R.A.S., 322, 438

Deich, W.T.S. 1986, M.S. Thesis, Cornell Univ. (D86)

Deich, W.T.S., Cordes, J. M., Hankins, T. H., & Rankin, J. M. 1986, Ap.J., 300, 540 (DCHR)

Downs, G. S. 1979, *Ap.J. Suppl.*, 40 365

Dyks, J., Rudak, B. & Harding, A. K., 2004, Ap.J., 607, 939

Everett, J. E., & Weisberg, J. M. 2001, Ap.J., 553, 341 (EW)

Gangadhara, R.T., & Gupta, Y. 2001, Ap.J., 555, 31

Gil, J.A., Kijak, J., & Seiradakis, J.H. 1993, A&A, 272, 268

Gil, J.A, Lyne, A.G., Rankin, J.M., Snakowski, J.K., & Stinebring, D.R. 1992, A&A, 255, 181

Gil, J. A., & Lyne, A. G. 1995, M.N.R.A.S., 276, 55.

Gil, J. A., Melikidze, G. I., & Mitra, D. 2002, A&A, 388, 246.

Gil, J. A., Lyubarsky, Y., & Melikidze, G. I. 2004, Ap.J., 600, 872.

Gould, M. & Lyne, A, 1998, M.N.R.A.S., 301, 235 (GL)

Gupta, Y., & Gangadhara, R.T. 2003, Ap.J., 584, 418

Gupta, Y.; Gothoskar, P., Joshi, B. C., Vivekanand, M.; Swain, R., Sirothia, S.& Bhat, N. D. R., 2000, ASP Conf. Ser. 202: IAU Colloq. 177: Pulsar Astronomy - 2000 and Beyond, 227

Hamilton, P. A., McCulloch, P. M., Ables, J. G., & Komesaroff, M. M. 1977, M.N.R.A.S., 180, 1 (HMAK)

Hankins, T. H., & Rankin, J. M. 2008, A.J., in press

Hankins, T. H., & Wolszczan, A. 1987, Ap.J., 318, 410 (HW)

von Hoensbroech, A., & Xilouris K. 1997, A&A Suppl., 126, 121 (vHX)

von Hoensbroech, A. 1999, Ph.D. thesis, Univ. of Bonn (vH)

Johnston, S., Hobbs, G., Vigeland, S., Kramer, M., Weisberg, J. M., & Lyne, A. G. 2005, M.N.R.A.S., 364, 1397 (J-05)

Johnston, S., Karastergiou, A. & Willett, K. 2006, M.N.R.A.S., 369, 1916 (JKW)

Johnston, S., Kramer, M., Karastergiou, A., Hobbs, G., Ord, S. & Wallman, J. 2007, M.N.R.A.S., 381, 1625 (J-07)

Johnston, S., Karastergiou, A., Mitra, D & Gupta, Y, 2008, M.N.R.A.S., 388, 261

Karastergiou, A. & Johnston, S. 2006, M.N.R.A.S., 365, 353 (KJ)

Karastergiou, A. & Johnston, S. 2007, M.N.R.A.S., 380, 1678

Kloumann, I. M., & Rankin, J. M. 2010, M.N.R.A.S., in press

Komesaroff, M.M. 1970, Nature, 225, 612

Kramer, M. 1994, A&A Suppl.107, 527

Kuzmin, A. D., Izvekova, V. A., Shitov, Yu. P., Sieber, W., Jessner, A., Wielebinski, R., Lyne, A. G., & Smith, F. G. 1998, A&A Suppl., 127, 355 (K-98)

Kuz'min, A. D. & Losovskii, B. Y. 1999, *Astr. Repts.*, 43, 288 (KL)

Lyne, A.G. 1990, private communication (L90)

Lyne, A.G., & Manchester, R.N. 1988, M.N.R.A.S., 234, 477 (LM)

Malofeev, V. M., Izvekova, V. A., & Shitov, Yu. P. 1986, preprint FIAN USSR (MIS)

Malov, I. F., & Suleimanova, S. A. 1998, Astr. Rpts. 42, 388

Manchester, R.N., Hamilton, P.A., & McCulloch, P.M. 1980, M.N.R.A.S., 192, 153 (MHM)

Manchester, R.N., Han, J.K., & Qiao, G.J. 1998, M.N.R.A.S., 295, 280 (MHQ)

McCulloch, P.M., Hamilton, P.A., Manchester, R.N., & Ables, J.G. 1978, M.N.R.A.S., 183, 645 (MHMA)

McCulloch, P.M., Hamilton, P.A., & Manchester, R.N. 1982, private communication (MHMb)

Mitra D & Deshpande A. A., 1999 A&A, 346, 906

Mitra, D, Gupta, Y. & Kudale, S., 2005, "Polarization Calibration of the Phased Array Mode of the GMRT", URSI GA 2005, Commission J03a

Mitra, D. & Rankin, J. M. 2002, Ap.J., 557, 322 (Paper VII)

Mitra, D., & Li, X. H., 2004, A&A, 421, 215

Mitra, D., Rankin, J. M. & Gupta, Y. 2007, M.N.R.A.S., 379, 932

Morris, D., Sieber, W., Ferguson, D. C. & Bartel, N., 1980, A&A, 260, 262

Morris, D., Graham, D.A., Sieber, W., Bartel, N., & Thomasson, P. 1981, A&A, 46, 421 (MGSBT)

van Ommen, T.D., D'Alessandro, F., Hamilton, P.A., & McCulloch, P.M. 1997, M.N.R.A.S., 287, 307 (vO97)

Radhakrishnan, V., & Cooke, D. J. 1969, Ap. Lett, 3, 225

Radhakrishnan, V., & Rankin, J. M., 1990, Ap.J., 352, 258

Ramachandran, R., Backer, D.C., Rankin, J.M., Weisberg, J.M., & Devine, K.E. 2004, Ap.J., 606, 1167

Rankin, J.M. 1983a, Ap.J., 274 333 (Paper I)

Rankin, J.M. 1983b, Ap.J., 274 359 (Paper II)

Rankin, J.M. 1986, Ap.J., 301, 901 (Paper III)

Rankin, J.M. 1988, Ap.J., 325, 314

Rankin, J.M. 1990,Ap.J., 352, 247 (Paper IV)

Rankin, J.M. 1993, Ap.J., 405, 285 and A&A Suppl., 85, 145 (Paper VI)

Rankin, J.M. & Ramachandran, R., 2003, Ap.J., 590, 411 (Paper VIII)

Rankin, J.M., Rodriguez, C., & Wright, G.A.E. 2006a, M.N.R.A.S., 370, 673 (RRW)

Rankin, J.M., Ramachandran, R., & Suleymanova, S.A. 2006b, A&A, 447, 235 (RRS)

Rankin, J.M., Ramachandran, R., van Leeuwen, J., & Suleymanova, S.A. 2006c, A&A, 455, 215 (RRvLS)

Rankin, J. M., Stinebring, D. R., & Weisberg, J. M. 1989, Ap.J., 346, 869 (RSW)

Ruderman, M.A. & Sutherland, P.G. 1975, Ap.J., 196, 51

Seiradakis, J. M., Gil, J. A., Graham, D. A., Jessner, A., Kramer, M., Malofeev, V. M., Sieber, W., & Wielebinski, R. 1995, aaps, 111, 205. (S95)

Sturrock, P. A. 1971, Ap.J., 164, 529.

Suleymanova, S. A., Volodin, Yu. V., & Shitov, Yu. P. 1988, Astro. Zh., 422, 17 (SVS)

Suleymanova, S. A., & Shitov, Yu. P. 1994, Ap.J., 422, 17 (SS)

Sirothia, S. 2000, M.Sc. thesis, University of Pune

Stairs, I. H., Thorsett, S. E. & Camilo, F., 1999, Ap.J., 123, 627

Swarup, G., Ananthakrishnan, S., Kapahi, V. K., Rao, A. P., Subrahmanya, C. R., Kulkarni, & V. K. 1991, Current Science 60, 95.

Weisberg, J. M., Cordes, J. M., Lundgren, S. C., Dawson, B. R., Despotes, J. T., Morgan, J. J., Weitz, K. A., Zink, E. C., & Backer, D. C. 1999, *Ap.J. Suppl.*, 121, 171 (W-99)

Weisberg, J. M., Cordes, J. M., Kuan, B., Devine, J. E., Green, J. T., & Backer, D. C. 2004, *Ap.J. Suppl.*, 150, 317 (W-04)

Weltevrede, P., Edwards, R. T., & Stappers, B. W. 2007, A&A, 469, 607 (WES)

Weltevrede, P., Stappers, B. W., & Edwards, R. T. 2006b, A&A, 445, 243 (WSE)

Weltevrede, P., Wright, G.A.E., Stappers, B. W., Rankin, J. M. 2006a, A&A, 458, 269 (WWSR)

Weltevrede, P., & Wright, G.A.E. 2009, M.N.R.A.S., 395, 2117 (WW09)

Wu, X.J., Manchester, R.N., Lyne, A.G., & Qiao, G.J. 1993, M.N.R.A.S., 261, 630 (WMLQ)

Xilouris, K.M., Rankin, J.M., Seiradakis, J.M., & Sieber, W. 1991, A&A, 241, 87 (XRSS)

Xilouris, K. M., Seiradakis, J. H., Gil, J., Sieber, W., & Wielebinski, R. 1995, A&A, 293, 153 (X-95)

Xilouris, K. M., Kramer, M., Jessner, A., von Hoensbroech, A., Lorimer D, Wielebinski, R., Wolszczan, A. & Camilo, F., 1998, Ap.J., 501, 286

The following is a list of the pulsars mentioned to comply with AASTEX§2.15.3. It doesn't print in the right place. B0138+59 B0254−53 B0355+54 B0450+55 B0540+23 B0647+80 B0740−28 B0809+74 B0906−17 B0919+06 B1055−52 B1112+50 B1221−63 B1240−64 B1322+83 B1356−60 B1426−66 B1449−64 B1530+27 B1530−53 B1540−06 B1556−44 B1604−00 B1612+07 B1641−45 B1648−42 B1700−18 B1732−07 B1742−30 B1745−12 B1756−22 B1822−09 B1842+14 B1851−14 B1859+07 B1900+05 B1907−03 B1910+20 B1913+10 B1915+13 B1924+16 B1930+22 B1937−26 B1944+17 B1944+22 B2021+51 B2043−04 B2053+36 B2217+47 B2224+65 B2327−20

This 2-column preprint was prepared with the AAS LATEX macros v5.0.

APPENDIX: Results for Individual Pulsars

B0138+59 presents an excellent example of a partial-cone profile in LM's intended sense. As in the 325 MHz PS in Figure A1 and LM:fig. 6, we mainly see the central and trailing parts of what could be a conal double (**M**) or quadruple (**Q**) structure. Only at 100 MHz does the leading feature fully reveal itself in the Pushchino profiles (SVS, MIS, K-98, KL), making the full half-power width nearly 40°. This suggests an outer cone with a 1-GHz width of about 27°, and a core width can be estimated as some 6-7° constraining α to some 20°.

The PA traverse using the GMRT PS at 325 MHz can be fitted to obtain α and β values of 69° and –4.8° respectively. The SG point is well constrained and is shown as the zero longitude in Figure A1. We see no flared emission towards the profile edges; however the fluctuation spectrum shows a low frequency excess as has been reported by the WES/WSE analyses. Given that the existing 100-MHz profiles seem to reveal the bright leading feature, sensitive new observations at low frequencies are needed to investigate this missing area of emission.

B0254–53 seems to have a narrow, conal double (**D**) profile (MHM, MHMA, MHMb, MHQ, vO97) with a slightly stronger leading component above 1 GHz and the reverse below. Its profiles are nearly depolarized and the PPA information difficult to interpret. The sweep value given by L&M seems too steep; rather we use a value of –8°/° from the 278-MHz MHMb profile. In short, it is not clear why L&M regarded this pulsar as a "partial cone".

PSR B0355+54: The pulse profile at various frequencies (*e.g.*, LM, GL, Xilouris *et al* 1998) clearly show three components, and the pulsar is classified as a core single by R93 due to the domination of the bright central component over the weak conal outriders. L&M identifies this pulsar as a "partial cone" owing to its asymmetric profile at high frequencies with the SG point of PPA traverse lying towards the trailing edge of the profile. This is also apparent from the GMRT PS at 325 MHz in Figure A1, where the PPA track is clearly delayed with respect to the putative core-component peak. Now, we interpret this displacement of the SG as indicating that A/R plays a strong role in this pulsar's profile form. To fit the RVM to the displaced-PPA track, we use a two-way mode-separation technique (*e.g.*, Gil *et al* 1993). The fit yields angles α=50.4±5° and β=–4.8±1°, consistent with the previous findings of L&M and Rankin (1993). The SG point of the PPA track is obtained with an accuracy of ±0.5° and corresponds to the longitude origin in Fig. A1. Moreover, the width of the central core component is measured to be just over 9°, indicates that α is just over 40°.

Changes in PSR B0355+54's profile shape were noted earlier by Morris *et al* (1980) at 11 cm, where short averages were seen to change slowly from one profile mode to the other over an interval of about 1000 pulses. We see no such mode change in our observation. The pulsar, however, shows sudden "flarings" towards the pulse edges for about 2% of the total time. Flarings on the leading and the trailing edges of the profile are generally uncorrelated and without any obvious periodicity. The flared profile in Fig. A1 clearly shows what seem to be conal outriders, and its overall form can be well described in terms of the triple (T) or perhaps M class—therefore we use the hybrid designation arT/M.

Further the midway point of the peak of the outer components clearly leads the steepest gradient point by about 15°, and hence the core peak lags the midway point by about 3°. The overall geometrical evidence here can be understood by invoking effects of A/R (BCW as corrected by Dyks *et al* 2004). If we assume that the flared pulse profile illuminates the full polar cap, then the BCW model gives an emission height for the outer cone of around 494 km. Assuming that the central feature is of the core type, then its peak leads the SG point of the PPA traverse by 12° yielding a core emission height of about 390 km. These 325-MHz height estimates of a few hundred km's are quite reasonable when compared to the radio emission heights estimated in other pulsars.

PSR B0450+55: We have generally viewed this pulsar as having a triple (**T**) profile, and its bright component as a core feature marked by sense-changing circular polarization especially at high frequency (*e.g.*, vH, GL, MIS, LM, KL, K-98). However, L&M were correct to note its forward-shifted PPA traverse at meter wavelengths, such that A/R seems to displace its core well toward the leading edge of its profile. The RVM-fitted PPA

Table A1: Observational Parameters

PSR Bname	**Obs'y Band**	**MJD**	**length/ res (°)**	**Fig.**
B0138+59	GM:P	54399	1961/0.15	A1
B0355+54	GM:P	53780	13144/1.18	A1
B0450+55	GM:P	53245	2671/0.54	A1
B0540+23	AO:P	54015	2440/0.66	A1
B0740–28	GM:P	53781	3649/1.10	A2
B0809+74	GM:P	54399	940/0.14	A2
B0906–17	GM:P	54399	2256/0.46	A2
B0919+06	AO:L	52854	1115/0.43	A2
B1055–52I	GM:P	54537	16571/0.93	A3
B1112+50	GM:P	54399	2002/0.11	A3
B1322+83m	GM:P	54399	2700/0.28	A3
B1530+27	AO:P	53994	1032/0.33	A3
B1540–06	GM:P	54399	2129/0.26	A4
B1556–44	GM:P	53781	3629/0.72	A4
B1604–00	AO:L	53372	1605/0.22	A4
B1612+07	AO:P	53378	1094/0.31	A4
B1700–18	GM:P	54399	1917/0.23	A5
B1732–07	GM:P	54399	2015/0.42	A5
B1742–30	GM:P	54399	1975/0.50	A5
B1745–12	GM:P	53781	2740/0.47	A5
B1822–09	GM:P	54399	1962/0.24	A6
B1842+14	AO:P	53378	1600/0.46	A6
B1851–14	GM:P	54399	1079/0.16	A6
B1900+05	AO:L	54842	1045/0.39	A6
B1907–03	GM:P	54399	2035/0.37	A7
B1910+20	AO:L	53372	906/0.33	A7
B1913+10	AO:L	54538	2077/0.26	A7
B1915+13	AO:L	48918	4000/0.33	A7
B1924+16	AO:L	54538	2522/0.26	A8
B1930+22	AO:L	54540	54540/0.64	A8
B1937–26	GM:P	54399	1965/0.46	A8
B1944+17	AO:P	53966	7038/0.31	A8
B1944+22	AO:P	55276	932/0.35	A9
B2021+51	GM:P	54399	2282/0.35	A9
B2043–04	GM:P	54399	1993/0.12	A9
B2053+36	AO:L	52837	52837/0.42	A9
B2217+47	GM:P	54399	2243/0.34	A10
B2224+65m	GM:P	54399	2101/0.27	A10
B2327–20	GM:P	54399	1865/0.11	A10

Notes: Pulsars with Bnames in normal type appear in L&M's Table 4; those in italics are denoted as "Partial cones?" in their Table 5

Table A2: Parameters for Lyne & Manchester's "Partial Cone" Pulsars.

PSR Bname	PSR Jname	P_1 (s)	$\log(\tau)$ (yrs)	$\log(B)$ (G)	$\log(\dot{E})$ (erg s^{-1})	Fig.	Remarks
B0138+59	J0141+6009	1.223	7.69	11.85	30.93	A1	L
B0254–53	J0255–5304	0.448	8.37	11.07	31.11	—	U
B0355+54	J0358+5413	0.156	5.75	11.92	34.66	A1	T
B0450+55	J0454+5543	0.341	6.36	11.96	33.38	A1	T
B0540+23	J0543+2329	0.246	5.40	12.29	34.61	A1	T
B0643+80	J0653+8051	1.214	6.71	12.34	31.92	—	U
B0740–28	J0742–2822	0.167	5.20	12.23	35.16	A2	T
B0809+74	J0814+7429	1.292	8.09	11.67	30.49	A2	T
B0906–17	J0908–1739	0.402	6.98	11.72	32.61	A2	U
B0919+06	J0922+0638	0.431	5.70	12.39	33.83	A2	T
B1055–52I	J1057–5226	0.198	5.73	12.04	34.48	A3	T
B1112+50	J1115+5030	1.656	7.02	12.31	31.34	A3	U
B1221–63	J1224–6407	0.216	5.84	12.02	34.28	—	U
B1240–64	J1243–6423	0.388	6.14	12.13	33.48	—	U
B1322+83m	J1321+8323	0.670	7.27	11.80	31.87	A3	T
B1356–60	J1359–6038	0.128	5.50	11.96	35.08	—	U
B1426–66	J1430–6623	0.785	6.65	12.17	32.36	—	U
B1449–64	J1453–6413	0.179	6.02	11.85	34.28	—	U
B1530+27	J1532+2745	1.125	7.36	11.98	31.33	A3	U
B1530–53	J1534–5334	1.369	7.18	12.15	31.34	—	U
B1540–06	J1543–0620	0.709	7.11	11.90	31.99	A4	U
B1556–44	J1559–4438	0.257	6.60	11.71	33.38	A4	T
B1604–00	J1607–0032	0.422	7.34	11.56	32.21	A4	T
B1612+07	J1614+0737	1.207	6.91	12.23	31.72	A4	U
B1641–45	J1644–4559	0.455	5.56	12.49	33.92	—	U
B1648–42	J1651–4246	0.844	6.44	12.31	32.51	—	U
B1700–18	J1703–1846	0.804	6.87	12.08	32.12	A5	T
B1732–07	J1735–0724	0.419	6.74	11.86	32.81	A5	U
B1742–30	J1745–3040	0.367	5.74	12.30	33.93	A5	U
B1745–12	J1748–1300	0.394	6.71	11.85	32.89	A5	T
B1756–22	J1759–2205	0.461	5.83	12.36	33.64	—	U
B1822–09	J1825–0935	0.769	5.37	12.81	33.66	A6	T
B1842+14	J1844+1454	0.375	6.50	11.93	33.15	A6	U
B1851–14	J1854–1421	1.147	6.64	12.34	32.04	A6	U
(B1859+07)	J1901+0716	0.644	6.65	12.09	32.53	—	
B1900+05	J1902+0556	0.747	5.96	12.50	33.08	A6	U
B1907–03	J1910–0309	0.505	6.56	12.03	32.83	A7	U
B1910+20	J1912+2104	2.233	6.54	12.68	31.56	A7	T
B1913+10	J1915+1009	0.405	5.62	12.40	33.96	A7	U
B1915+13	J1917+1353	0.195	5.63	12.08	34.59	A7	T
B1924+16	J1926+1648	0.580	5.71	12.52	33.56	A8	T
B1930+22	J1932+2220	0.144	4.60	12.47	35.88	A8	T
B1937–26	J1941–2602	0.403	6.82	11.80	32.76	A8	T
B1944+17	J1946+1805	0.441	8.46	11.02	31.041	A8	U
B1944+22	J1946+2244	1.334	7.38	12.04	31.18	A9	U
B2021+51	J2022+5154	0.529	6.44	12.11	32.91	A9	T
B2043–04	J2046–0421	1.547	7.22	12.18	31.20	A9	—
B2053+36	J2055+3630	0.222	6.98	11.46	33.13	A9	U
B2217+47	J2219+4754	0.538	6.49	12.09	32.84	A10	U
B2224+65m	J2225+6535	0.683	6.05	12.41	33.08	A10	L
B2327–20	J2330–2005	1.644	6.75	12.45	31.61	A10	—

Notes: Pulsars with Bnames in normal type appear in L&M's Table 4; those in italics are denoted as "Partial cones?" in their Table 5; and one other star, B1859+07 (parentheses) is included from our own work. The periods (P_1), age ($\tau = P_1/2\dot{P}_1$), magnetic field (B) and energy are taken from the ATNF pulsar catalogue. The referenced figures appear in the Appendix, and the last column specifies if the SG point is either trailing (T) or leading (L) or unclear (U) *wrt* the pulsar profile and the (—) referes to cases where the SG point is consistant with being coincident with the profile center.

Table A3: Emission-Beam Geometry of “Partial Cone” Pulsars

			$\Delta\chi/\Delta\varphi$		Inner			Outer			r (km)	
PSR	Class	α	(°/°)	β	$\Delta\Psi$	ρ	β/ρ	$\Delta\Psi$	ρ	β/ρ	Inner	Outer
B0138+59	M/cQ?	**20**	**–11.2**	1.7	∼ —	—	—	27	5.1	0.34	—	211
B0254–53	D?	55	–8?	5.9	7	6.6	0.89	—	—	—	129?	—
B0355+54	arT/M	**42**	**–9.2**	4.2	—	—	—	40	14.6	0.29	133	221
B0450+55	arT	**32**	**–8.5**	3.5	—	—	—	34	10.0	0.35	127	226
B0540+23	arSt	**38**	**–3.4**	10.4	—	—	—	—	—	—	—	—
B0647+80	Sd?	22	+6	3.6	9	4.0	0.89	—	—	—	130	—
B0740–28	arM?	90?	**–5.5**	10.5	7?	11.0	0.95	18?	13.8	0.76	135	211
B0809+74	Sd	8.8	**–1.8**	4.9	—	—	—	17.0	5.1	0.95	—	227
B0906–17	arT	31	–6?	4.9	17?	6.8	0.73	—	—	—	124	—
B0919+06	arT	**53**	+9	5.1	10	6.5	0.78	—	—	—	122	—
B1055–52i	M?	**22**	**+9.1**	2.4	—	—	—	65?	13.1	0.18	–	224
B1112+50	St?	**30**	**+10.1**	2.8	7	3.4	0.84	—	—	—	126	—
B1221–63	T?	61	+7	7.2	13	9.3	0.77	—	—	—	125	—
B1240–64	St	69	+15	3.6	13?	7.1	0.50	—	—	—	131	—
B1322+83m	Sd?	**14**	**+2.8**	5.1	12?	5.4	0.95	—	—	—	130	—
B1356–60	St	**79**	+3[a]	19.1	—	—	—	—	—	—	—	—
B1426–66	T	**54**	–50[a]	0.9	12	5.0	0.19	—	—	—	131	—
B1449–64	St	**43**	+7[a]	5.6	25?	10.5	0.53	—	—	—	132	—
B1530+27m	Sd/D?	44	**–8.9**	4.4	—	—	—	9	5.4	0.82	—	222
B1530–53	D?	22	–18[a]	1.2	19?	3.8	0.31	—	—	—	128	—
B1540–06	Sd	59	–14?	9?	5.3	0.67	—	—	—	—	131	—
B1556–44	St/T	**32**	–9[a]	3.4	28	8.6	0.40	—	—	—	125	—
B1604–00	cT	50	–8?	5.5	9.8	6.7	0.82	—	—	—	128	—
B1612+07	Sd	25	–4.6	5.2	—	—	—	4.5	5.3	0.98	—	224
B1641–45	St	**33**	∞	0.0	24	6.5	0.0	—	—	—	128	—
B1648–42	D/cT	6.5	–4[a]	1.6	—	—	—	100	6.3	0.26	—	226
B1700–18	Sd	44	**–8.4**	4.7	—	—	—	12	6.4	0.74	—	221
B1732–07	T?	**54**	∞	0.0	17	6.8	0.0	—	—	—	131	—
B1742–30	M	**24**	–3.6	6.4	15?	7.3	0.89	32	9.7	0.67	129	228
B1745–12	T/cQ?	75	**–11.4**	4.9	—	—	—	16?	9.2	0.53	—	222
B1756–22	St/T?	∼90?	∞	0.0	12?	6.2	0.0	—	—	—	118	—
B1822–09m	T	**86**	∞	0.0	10.0	5.0	0.0	—	—	—	128	—
B1842+14	St?	63	+12	4.2	12	6.9	0.62	—	—	—	119	—
B1851–14	Sd?	34?	**–7.8**	4.1	—	—	—	12?	5.4	0.76	—	224
(B1859+07)	T/M?	30	+6	4.9	—	—	—	20	7.1	0.67	—	219
B1900+05	St?	59?	∞	0.00	12?	5.1	0.0	—	—	—	132	—
B1907–03	St/T	**44**	∞	0.0	18	6.2	0.0	—	—	—	129	—
B1910+20	cQ/M	**32**	**+30**	1.0	∼10.5	3	0.34	14	3.9	0.26	133	225
B1913+10	St?	**64**	?	—	—	—	—	—	—	—	—	—
B1915+13	arSt	68	**–9.8**	5.4	—	—	—	—	—	—	—	—
B1924+16	arSt	**34**	**+5.2**	6.2	—	—	—	—	—	—	—	—
B1930+22	arSt?	71	**+5.1**	10.7	10?	11.8	0.91	—	—	—	133	—
B1937–26	T?	**42**	**–4.5**	8.5	—	—	—	9	9.1	0.94	—	222
B1944+17	cT/cQ	**5**	**+0.8**	6.4	∼95?	8.9	0.72	30	6.7	0.95	—	131
B1944+22	Sd/D?	40	–12?	3.1	7?	3.8	0.80	—	—	—	132	—
B2021+51	Sd?	**30**	**+3.9**	7.3	—	—	—	10.3	7.8	0.93	—	216
B2043–04	Sd/D	73	**+27.1**	2.0	6?	3.5	0.57	—	—	—	128	—
B2053+36	St	**34**	∞	—	~~18~~	—	—	—	—	—	—	—
B2217+47	St	**42**	+8.5	4.5	12.0	6.1	.73	—	—	—	135	—
B2224+65m	St?	**27**	**+5.3**	—	—	—	—	—	—	—	—	—
B2327–20	T?	**66**	**+43**	1.2	7.0	3.4	0.35	—	–	–	128	—

Notes: Pulsars with Bnames in normal type appear in L&M’s Table 4; those in italics are denoted as “Partial cones?” in their Table 5; and one other star, B1859+07 (parentheses) is included from our own work. The α values in boldface were measured by fitting or other means; while the others were estimated from profile dimensions. The $\Delta\chi/\Delta\varphi$ values in boldface were determined by PPA fitting; the others were taken from Paper VI or the [a] values from L&M.

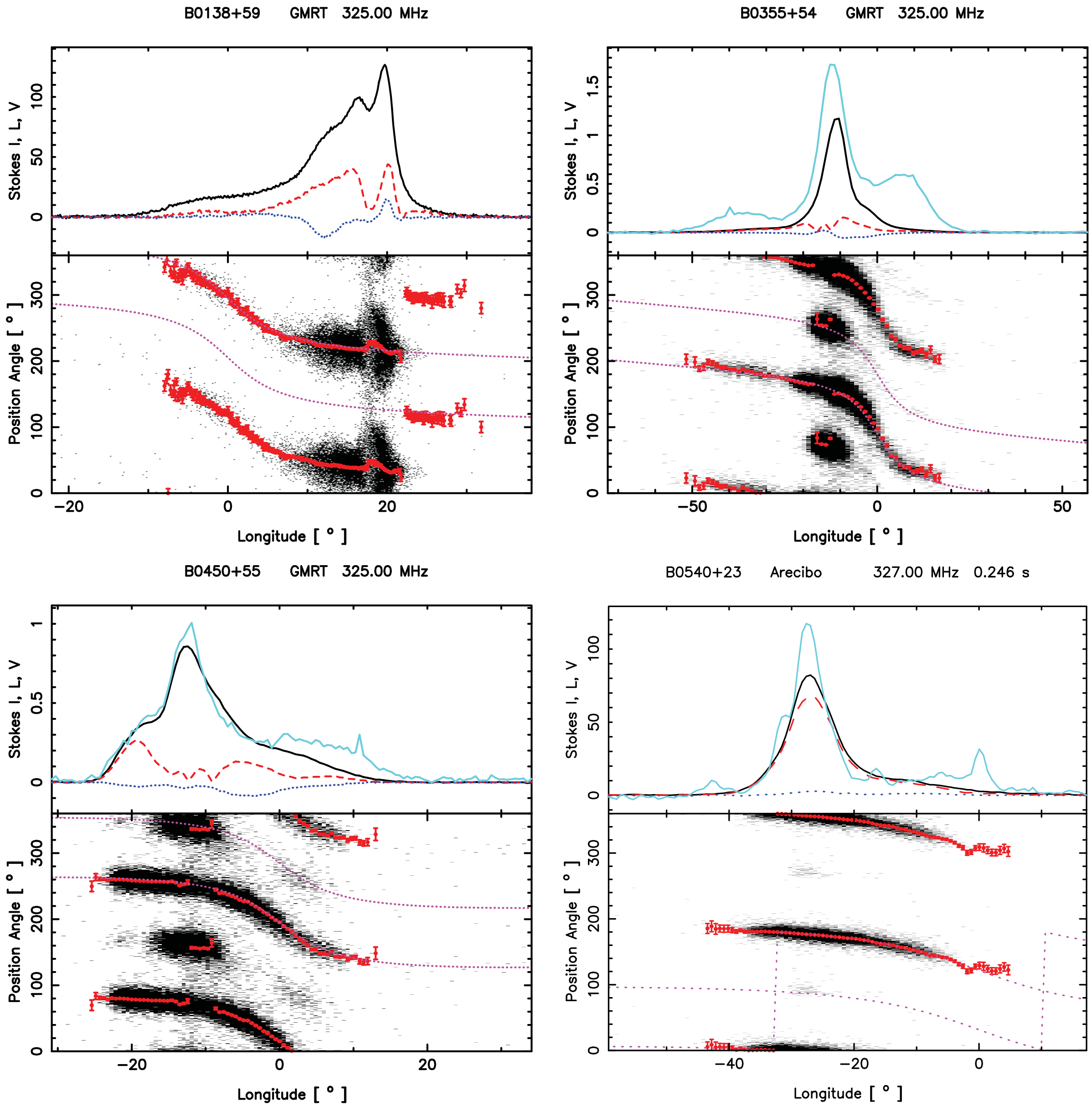

Fig. A1.— PPA histograms and "flared"-emission profiles for "partial cone" pulsars B0138+59, B0355+54, B0450+55 and B0540+23, where the instrument and band is indicated above each plot. The respective upper panels give the total power (black), total linear (red) and circular polarisation LH-RH (blue). The cyan curve (if plotted) correspond to the computed flared profile (see text for details). The lower panels give the polarization-angle (hereafter PPA) density, plotted twice for clarity. In cases where PPA fits were possible, the two dotted (magenta) curves indicate the primary- and secondary-mode (hereafter PPM and SPM) RVM fits to the PPA traverse. In these cases, the longitude origin is taken at the steepest gradient point (hereafter SG) given by the fits. Otherwise, when no RVM fitting information was available, the zero longitude was usually chosen as the peak of the profile (unless mentioned otherwise in notes on each pulsar in this Appendix).

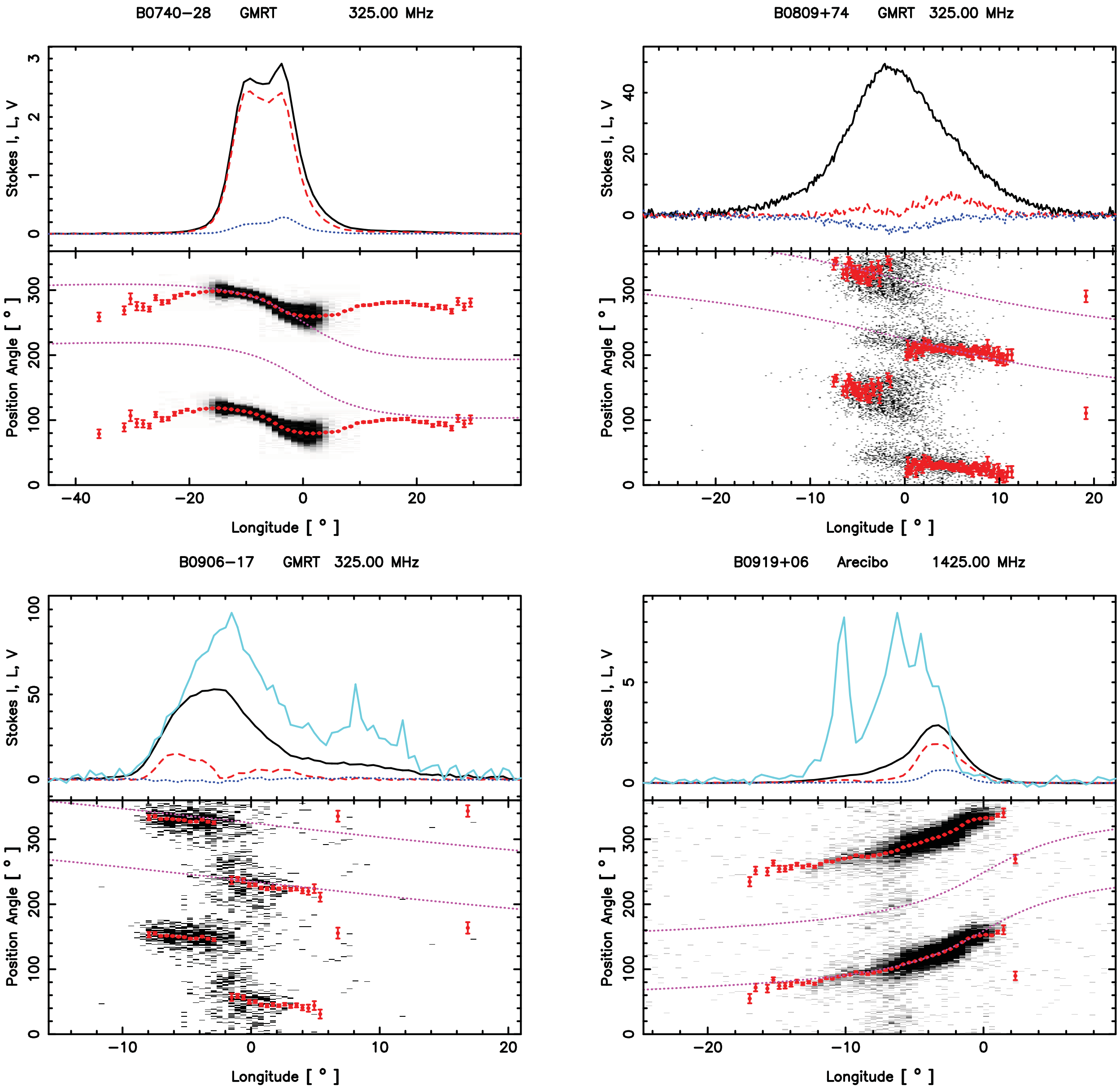

Fig. A2.— PPA histograms and "flared"-emission profiles as in Fig. A1 for pulsars B0740–28, B0809+74, B0906–17 and B0919+06.

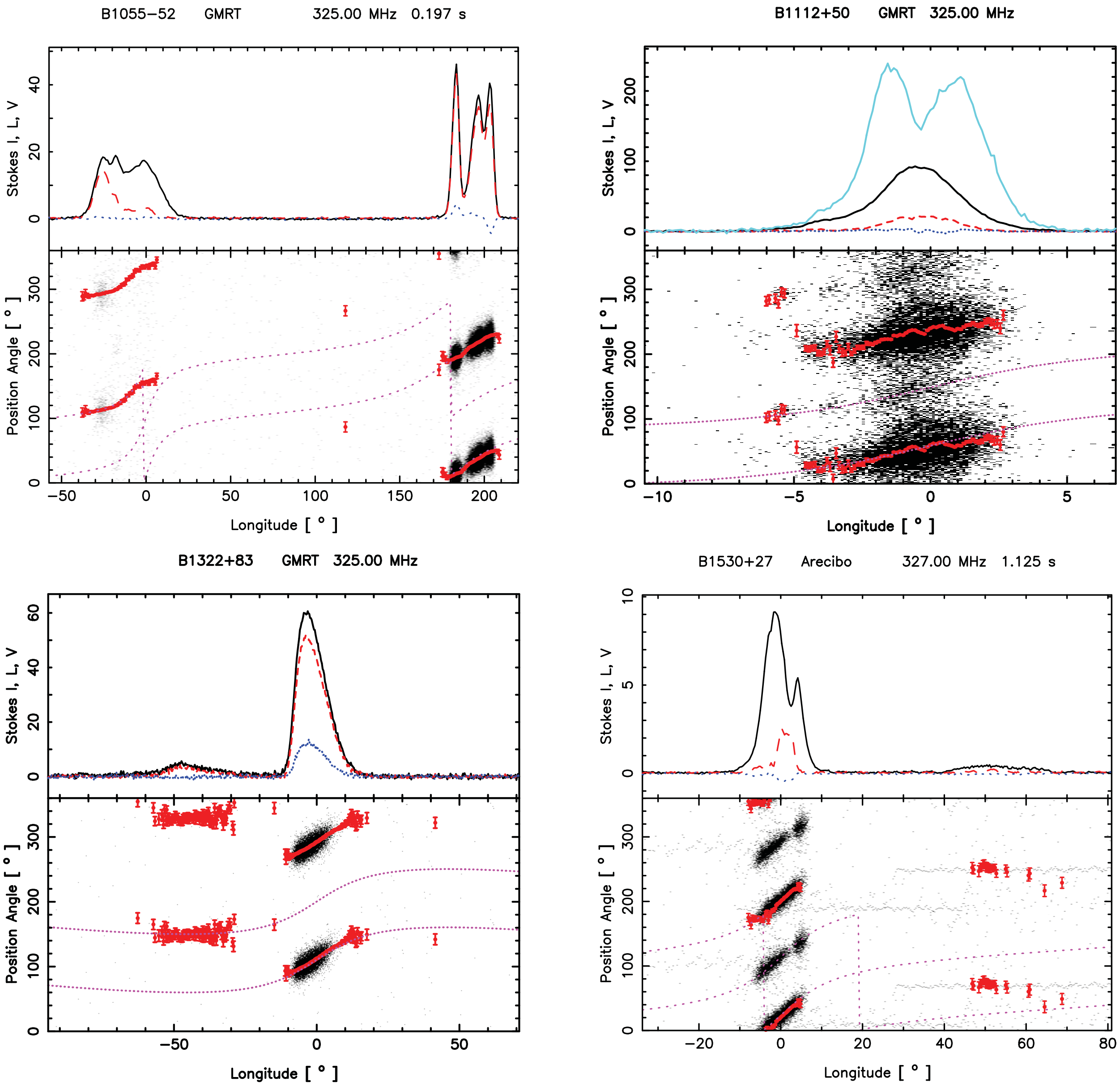

Fig. A3.— PPA histograms and "flared"-emission profiles as in Fig. A1 for pulsars B1055–52, B1112+50, B1322+83 and B1530+27.

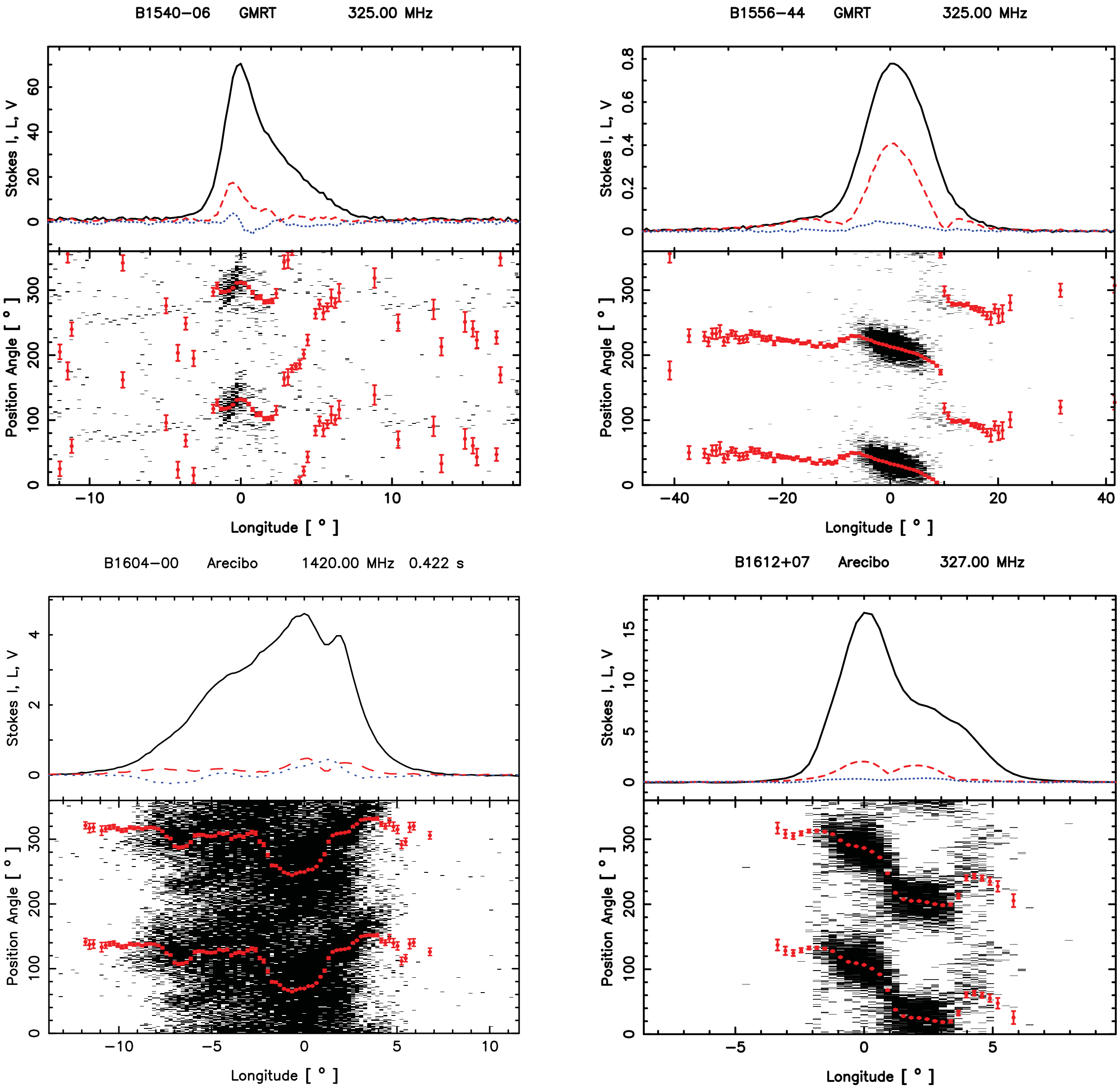

Fig. A4.— PPA histograms and "flared"-emission profiles as in Fig. A1 for pulsars B1540–06, B1556–44, B1604–00 and B1612+07.

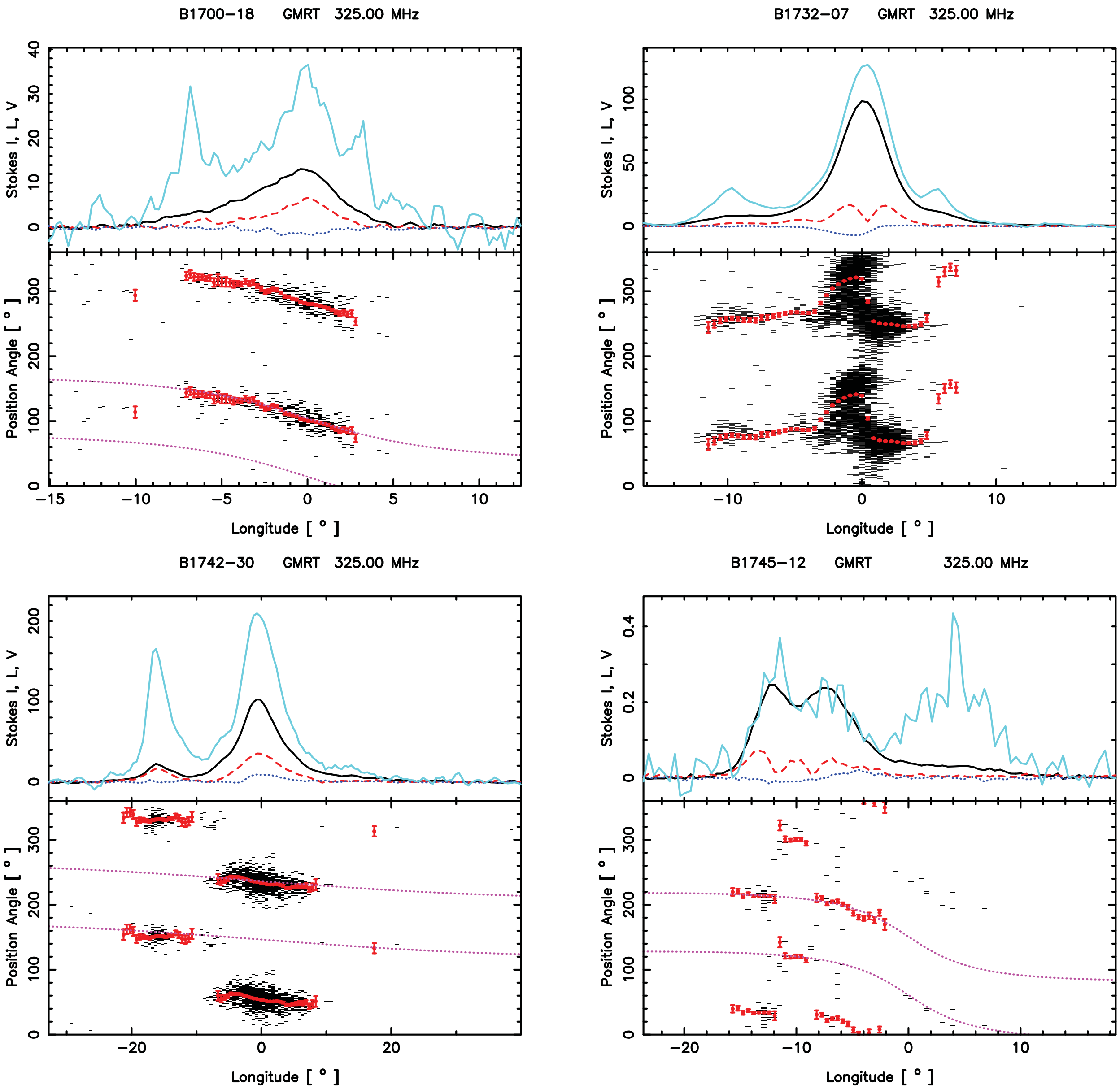

Fig. A5.— PPA histograms and "flared"-emission profiles as in Fig. A1 for pulsars B1700–18, B1732–07, B1742–30 and B1745–12.

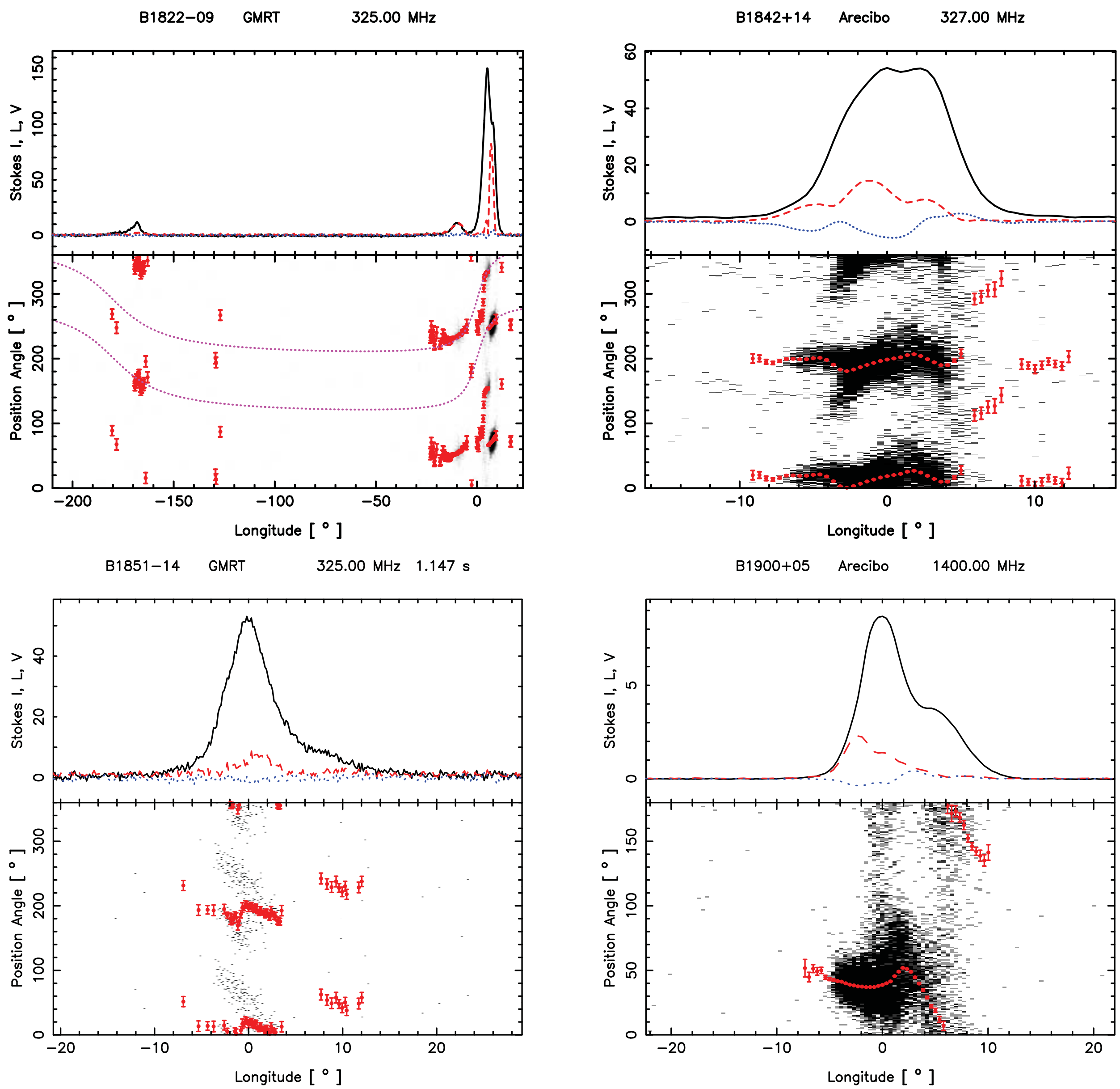

Fig. A6.— PPA histograms and "flared"-emission profiles as in Fig. A1 for pulsars B1822–09, B1842+14, B1851–14 and B1900+05.

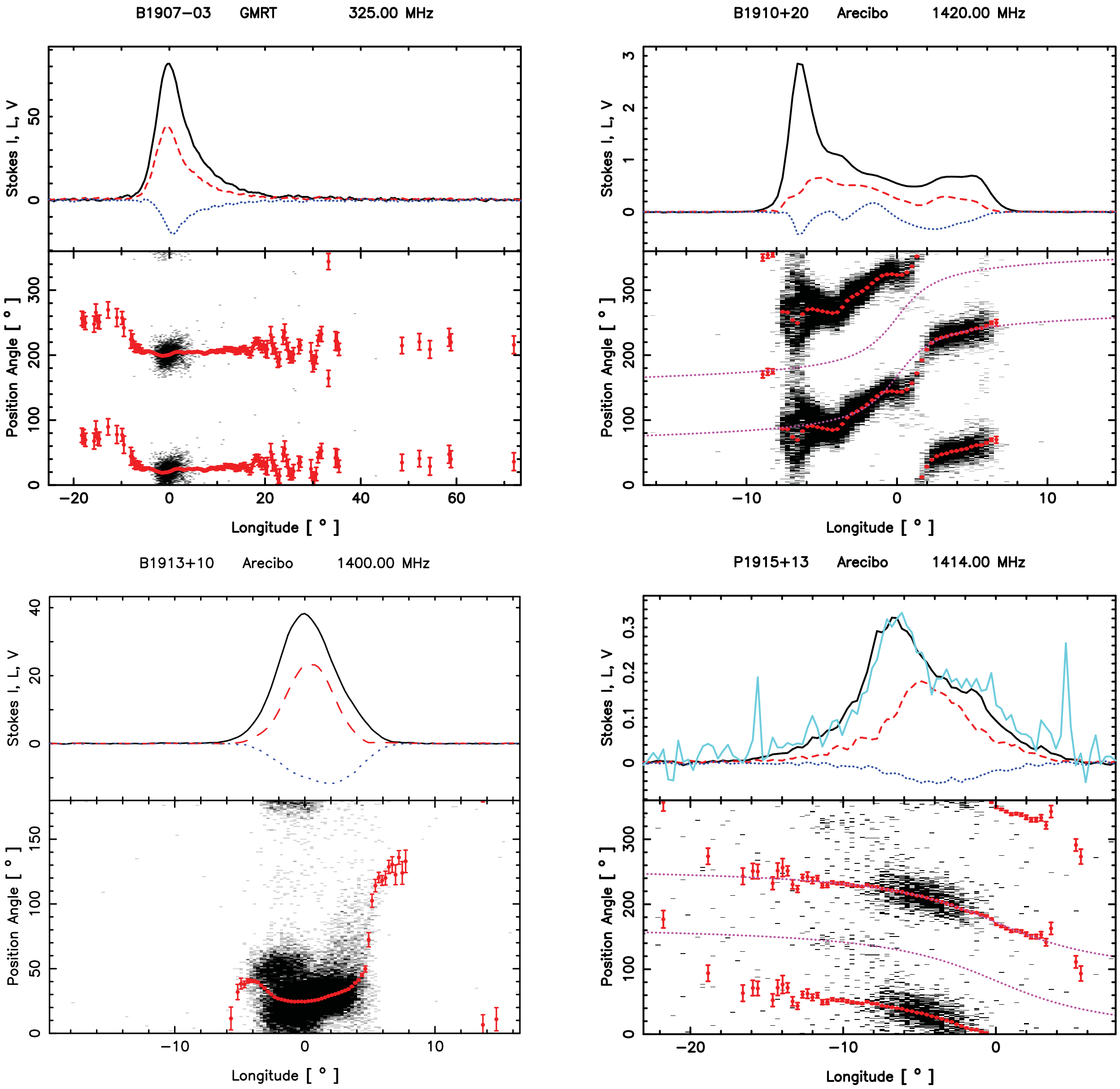

Fig. A7.— PPA histograms and “flared”-emission profiles as in Fig. A1 for pulsars B1907–03, B1910+20, B1913+10 and B1915+13.

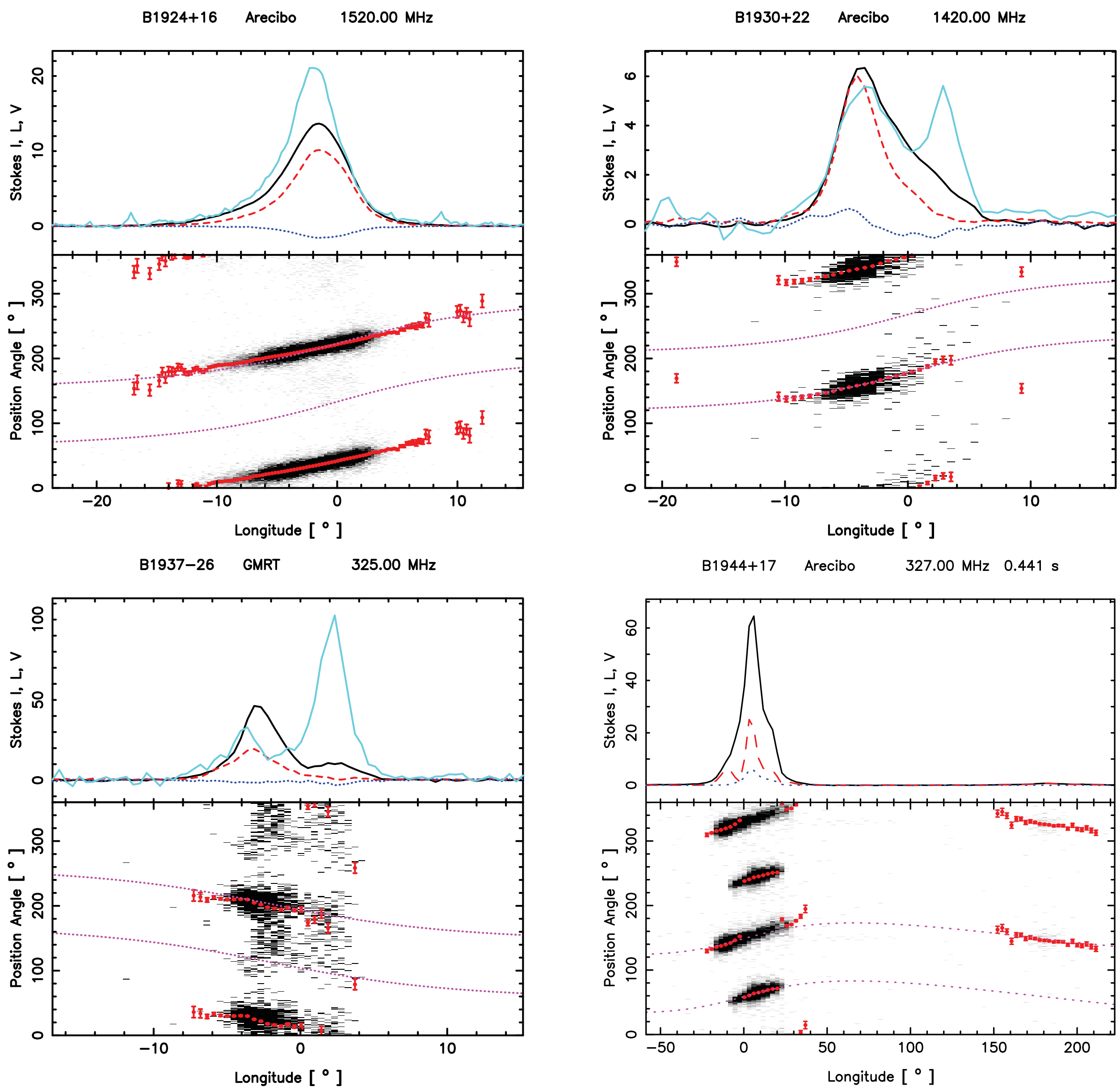

Fig. A8.— PPA histograms and "flared"-emission profiles as in Fig. A1 for pulsars B1924+16, B1930+22, B1937–26 and B1944+17.

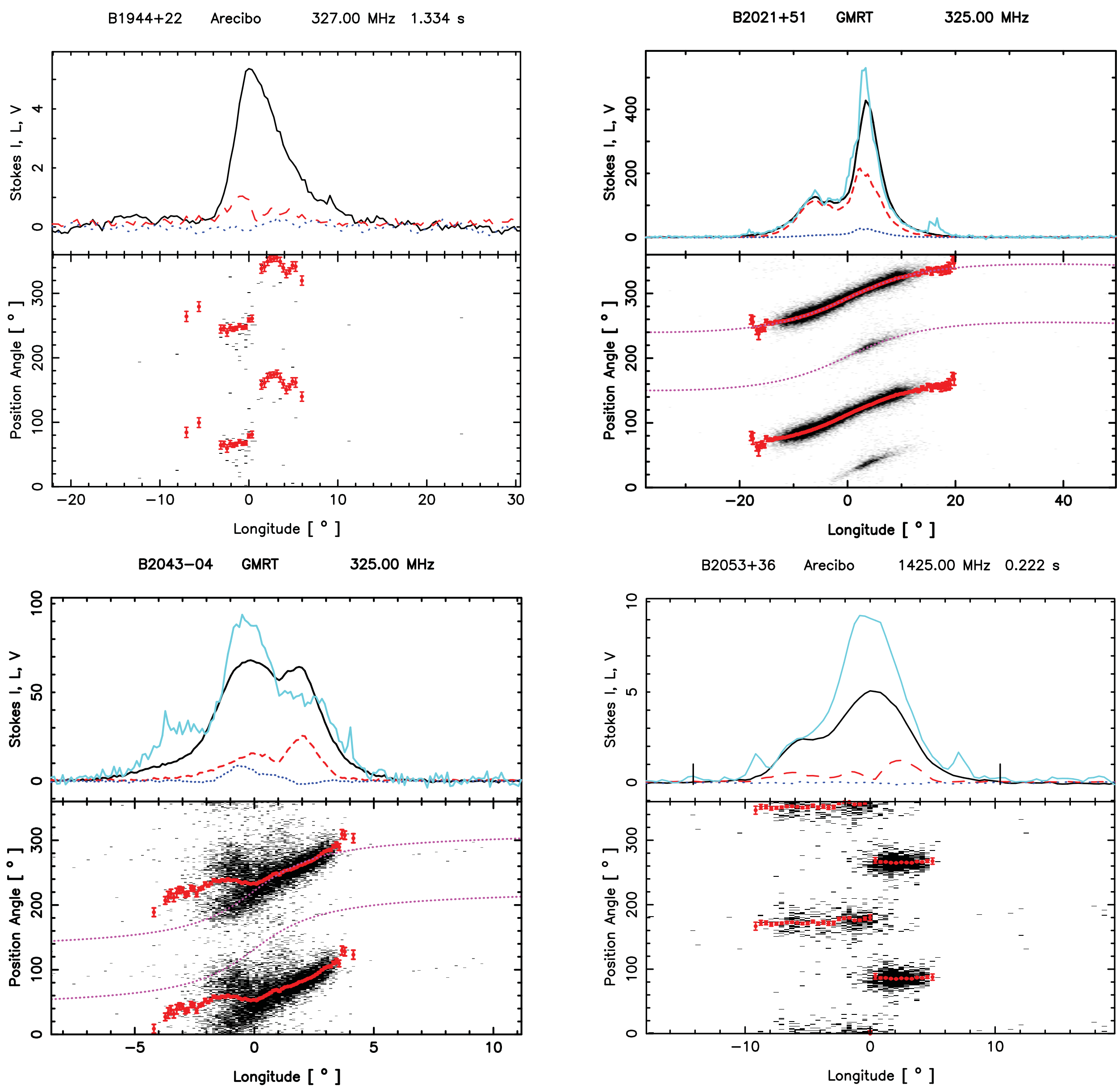

Fig. A9.— PPA histograms and "flared"-emission profiles as in Fig. A1 for pulsars B1944+22, B2021+51, B2043–04 and B2053+36.

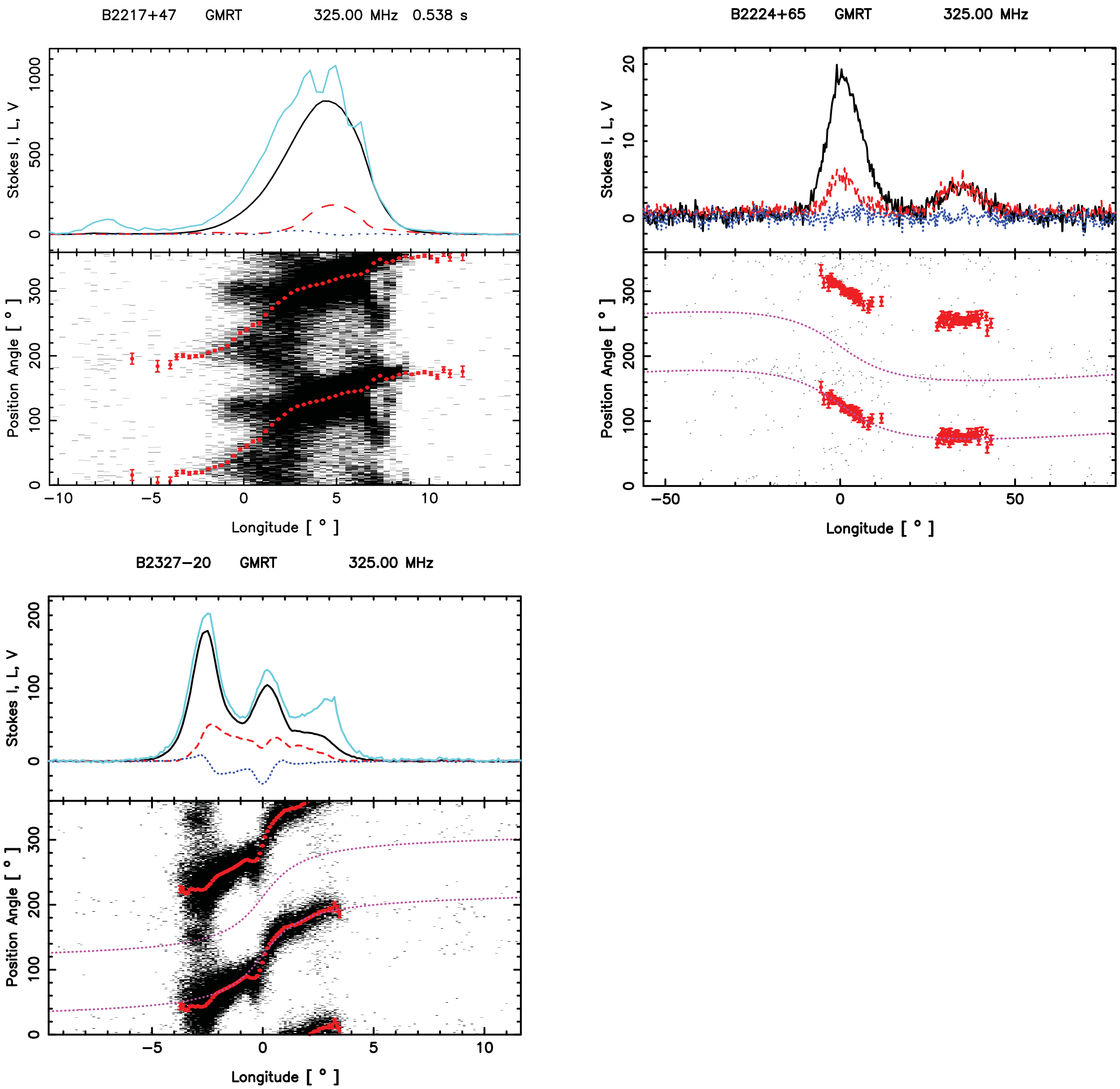

Fig. A10.— PPA histograms and "flared"-emission profiles as in Fig. A1 for pulsars B2217+47, B2224+65 and B2327–20.

Table A4: Table for A/R heights

PSR Bname	Period (sec)	Left width (°)	Right Width (°)	Shift/ (°)	Height (km)
0355+54	0.156	–39.7	9.3	15.2	494
0450+55	0.340	–18.5	10.8	3.9	275
0540+23	0.245	–42.5	-0.0	21.3	1087
1700–18	0.804	–6.6	3.3	1.6	279
1732–07	0.419	–10.0	5.3	2.3	205
1742–30	0.367	–16.2	13.9	1.1	87
1745–12	0.394	–12.0	6.8	2.6	215
1910+20	2.232	–6.4	5.4	0.5	228
1924+16	0.579	–17.0	8.6	4.2	506
1930+22	0.144	–10.6	4.2	3.2	96
1937–26	0.402	–3.9	2.2	0.8	71
2021+51	0.529	–18.3	16.2	1.0	113
2043–04	1.546	–3.5	4.1	-0.2	—
2327–20	1.643	–2.6	3.0	-0.1	—

Notes: The table gives the pulsar name, period, measured outer conal left and right widths and the shift w.r.t the SG point which is at zero longitude. The estimated A/R heights are given in the last column.

traverse gives α=133±7° and β=-4.9±2°, and the angles are highly correlated. The SG point is the longitude origin in Figure A1 with an error of about 1°. The about 8° width of the core at near 1 GHz also constrains α to some 30°. Therefore, here we designate the pulsar as having an arT profile.

Fig. A1 shows the pulsar's profile at 325 MHz, where the green curve shows the "flaring" character of the emission on the far trailing edge of the profile, something also seen via the large modulation index in the WES/WSE analysis. The regions immediately adjacent to the bright feature show strong stationery 9.5-P_1 modulation, suggesting that they are conal. The flared profile gives clear indication of the leading and trailing conal emission, and we can use the edges of the outermost cone to estimate the midway point of the profile which leads the SG point by about 3.9°, in turn giving an emission height of about 275 km. This reasonable height estimate for the conal emission supports the conclusion that A/R plays a strong role in the profile evolution.

PSR B0540+23, with its steeply rising profile, long trailing "tail" and flat to steep PPA traverse, is one of LM's classic "partial cone" objects. Moreover, this behavior is progressive over a very broad band from some 0.3 to 10 GHz (RSW, GL, W-99, W-04, vHX, TR, X93, J-07, BCW), such that at very high frequency the profile has a nearly Gaussian form and an ever more extended "tail" at longer wavelengths. Further, the star's PPA traverse is consistently flattish on the leading side of the profile and rotates ever more steeply downward in the trailing region—a clear indicator of A/R. Careful inspection reveals that the PPA SG point lags the profile peak ever farther at lower frequencies; for example, at 10.5 GHz the SG point falls under the symmetrical profile, whereas at 430 MHz the peak leads the SG point by more than 20°! B0540+23's profile evolution then appears to provide a "textbook" example of A/R displacement such that the backward emission shift of the bright component is roughly proportional to wavelength. In turn, this interpretation requires that the emission height increase progressively with wavelength.

Further, assuming that the bright feature is a core component, its 1-GHz width is just less that 8° arguing that α is about 38°. Overall, we find little evidence for conal emission in the star's profiles: no "outriders" are seen at high frequency, no regular features are seen in the fluctuation spectra (WES/WSE), and the weak "flaring" on the extreme profile edges does not seem compatible with conal beam dimensions. In some low frequency profiles, the trailing "tail" does suggest an unresolved second component (*e.g.*, see GL's profiles at 408 and 234 MHz); however, our 327-MHz observation in Figure A1 shows little hint of this feature, so this behavior may not be consistent. In any case, if A/R is so strongly active in profiles like that of B0540+23—suggesting high altitude *core* emission as documented in B0329+54—then it is possible that any conal features are smeared or overridden by the shifting core emission.

In Paper VI this pulsar was classified as having core-single ($\mathbf{S}_t$) profile, and this identification may yet be correct. However, A/R effects clearly dominate this star's profile evolution—producing the backward shift with wavelength and perhaps smearing any conal features—so we note this circumstance with an "ar" to give this pulsar the hybrid designation ar$\mathbf{S}_t$. The PPA traverse in Fig. A1 is well fitted by α and β values of 118.8°and –14.9°, respectively, giving a maximum sweep rate of –3.4°/°. The midway point of the flared profile leads the SG point by about 21°, giving an A/R height of 1087 km. This estimate is somewhat higher than usual emission heights of a few hundred km in pulsars, and might be indicative of missing conal emission.

B0643+80: Profiles for this pulsar have been published spanning 100 MHz to 5 GHz (GL, vH, MIS, S95). Most of these show a bright leading and weak trailing component; however, at 102 MHz this configuration is reversed, perhaps due to a second mode (MIS). The profile exhibits a nearly constant half power width of about 9° over this large frequency range, and the PA sweep rate can be estimated from GL's 1.4-GHz profile. Overall, the pulsar appears to show a conal single evolution that is quite reminiscent of B0943+10. WSE report that the star's fluctuation spectra are featureless at 92 cm. It is thus unsurprising that L&M classed this pulsar as having a "partial cone" profile.

PSR B0740–28 is yet another example of a "partial cone" in the L&M sense, apparently owning to the displacement of its PPA SG point on the trailing side of its profile—probably indicative, we now know, of A/R effects. Its average profiles show significant pulse-shape evolution with frequency (*e.g.*, vH, MHQ, GL, J-05, KJ, JKW),[3] and as many as seven components are needed to fit its profile at 1.4 GHz (Kramer 1994).

In Figure A2 we show the average Stokes profile and grey-scale PPA histogram of the 325-MHz pulse from the GMRT PS. Using a similar analysis as for B0355+54, we failed to find any evidence for "flaring" on the profile edges. Unfortunately, this high S/N profile does resolve the PPA traverse any farther into the "wings" than the previous observations.

More clarifying are the LRF spectra for this pulsar (Fig. 2), computed from the above PS, that exhibit a narrow 3.6 c/P_1 fluctuationfeature on the edges of its profile—suggesting that the pulsar illuminates the entire annular region around its magnetic axis and that its profile edges correspond to the outer edges of this region. No such feature was reported by WES/WSE; but it is possible that such "drifting" intervals are episodic (as for pulsar B1944+17 below), and this may account for the pulsars's profile instability as well.

The PPA fit corresponding to α and β of 173 and –1.3° gives a maximum sweep rate of –5.5°/° with the resultant SG point at the indicated longitude origin. The star's several components (*i.e.*, see KJ's profiles at 1.4 and 3.1 GHz) can only be understood quantitatively as a core/double structure if its magnetic geometry is nearly orthogonal, such that the inner and outer conal components have outside dimensions of something like 9 and 18°, respectively. We then designate this pulsar as having an arM profile.

B0809+74 presented the initial example of profile "absorption" (Bartel *et al* 1981, Bartel 1981). A review of the many consequences as well as modern efforts to understand the effects appears in RRS/RRvLS, which show that the longitude of the magnetic axis at meter wavelengths falls on the leading edge of the profile at about the half-power point. Our GMRT profile in Figure A2 shows the "absorbed" 325-MHz form, such that the full profile would have a half-power width of some 17°. Here, the PPA fit (with α=32°and β=-8.8°) does not properly locate the fiducial longitude—which here would fall about –7°—and the PPA "jump"

[3]Some of the older published profiles (*i.e.*, MHMA, MHM, MHMb, MGSBT, vO97, even GL) show little detail and thus do not seem to have been resolved adequately.

is modal in origin. Despite its "absorption" the star's profile and frequency evolution is characteristic of the conal single ($\mathbf{S}_d$) class, and A/R effects seems to play no significant role.

B0906–17: As seen in Figure A2 the pulsar exhibits a sharply rising profile with a long weak trailing tail as well as a PPA traverse that steepens to the SG point only on the trailing edge of the profile, prompting L&M to regard it as having "partial cone" emission. We also see evidence of sporadic emission across the entire profile. More recent work (XRSS, vH, GL) often resolves a trailing component, and the 21-cm profiles (see J-05) show a leading-edge inflection that suggests a third. The asymmetrically curved PPA traverse (with a prominent 90° "jump") steepens steadily with longitude and strongly suggests A/R. Unfortunately, the WES/WSE analyses are not very revealing in this case. The overall evidence then suggests that the star's profile might be regarded as A/R triple (ar**T**), such that this structure is obscured at low frequency, because A/R moves the central (putative core) component to ever earlier longitudes. The PPA fit in Fig. A2 (with α=36°and β=-15°) is neither able to measure the maximum sweep rate nor to locate the PPA inflection point. That the sweep rate here is far too shallow is clear by reference to the 1.4-GHz profile of J-05.

B0919+06: Figure A2 L&M classify this pulsar as a "partial cone" with its SG point lying towards the trailing part of its profile. The star's average emission shows a long dim ramp proceeding its bright trailing component, and it exhibits very similar profiles in form and dimensions over the 0.1 to 10.6-GHz range of the existing observations. A recent single pulse polarimetric study (Rankin *et al* 2006a) found that the dimmer leading parts of the profile can suddenly brighten up for several tens of pulses and then revert back to their normal faintness (see their Figs. 1 and 3). The effect is similar to the "flaring" event seen for PSR B0355+54 discussed earlier, and here the above study demonstrated that the overall profile is triple (T) with both core and conal dimensions scaling in terms of the polar-cap size. The fluctuation spectra provide (see WES/WSE) little insight for this star.

The 325-MHz PS in Rankin *et al* (2006): fig. 3 clearly shows that the PPAs exhibit strong OPMs mostly towards the leading parts of the profile. The average PPAs thus show a complicated behaviour which probably led LM88 to conclude that the SG point is towards the leading edge of the profile. Here, we have used the same 1400-MHz PS as in the above study to fit the RVM to the PPA traverse. The PPA at this frequency is mostly dominated by a single OPM. Our fit yields values of α=162.0 and β=+1.5°—giving a maximum sweep rate of +11.8°/°. The fitted PPA traverse is shown in Fig. A2 with the longitude origin falling at the SG point towards the trailing edge of the profile. The above sweep rate is flatter and more linear than that seen at meter wavelengths; therefore, we have retained the model values from the above study in Table A3 (see also BCW's profiles). Clearly the star's PPA behavior is consistent with an A/R signature as predicted by the BCW model—so we designate it as having an arT profile—although its overall effect is not at all clear.

B1055–52I: This prominent southern interpulsar has been studied by many investigators (HMAK, MHMA, vO97, Biggs 1990, MHMb, LM, CMH) and the configurations of its main pulse and interpulse widely debated. By far the most comprehensive treatment has been given in the recent paper by Weltevrede & Wright (2009). These authors find a nearly orthogonal geometry (α=75°) as have several other groups including ourselves (see Figure A3). They also support the idea that a trailing portion of the star's interpulse is missing, as did L&M in arguing that it was a "partial cone". Our RVM fits yield α=101°and β=7.2°.

B1112+50: At meter wavelengths this pulsar has an asymmetric single profile, and it is apparently on this basis that L&M regarded it as a "partial cone". Above 1 GHz the star's profile consists of two components which are at times well resolved and sometimes not, indicating several modes. Profiles and polarimetry are available by a number of authors (MGSBT, GL, L90, XRSS, KL, MIS), and both modal and fluctuation studies are available by Wright *et al* (1986) and WES/WSE. Our 325-MHz GMRT observation is shown in Figure A3, which shows both its asymmetric single profile and "flared" double form. The LRFs show only weak periodic modulation, but the star's PS are highly modulated at both frequencies in the WES/WSE analyses. Overall, the profile evolution appears conal, though the forms may entail some core emission in the profile center at lower frequencies. In any case, the PPA fitting in Fig. A3 yields $\alpha = 11.1$ and $\beta = 1.1$, giving a sweep rate of 10°/° and a poorly determined SG point. This together with the profile width and an estimate of the putative core dimension suggest the inner cone geometry in Table A3.

B1221–63: Here, we do not understand why L&M regarded this pulsar as a "partial cone". Profile polarimetry of uneven quality is available over a band from 0.27 to 1.6 GHz (MHM, MHMA, MHMb, vO97, WMLQ). Overall, the pulsar seems to exhibit a triple form (MHM), and estimates of the profile and core widths together with the sweep rate suggest an inner cone geometry as seen in Table A3.

B1240–64: This pulsar has a symmetrical single profile below 1 GHz, though some of the observations are poorly resolved (MHMA, CMH, vO97). It was probably the leading "ramp" on MHM's 1.6 GHz observation that pushed this star into L&M's "partial cone" category. Surely, KJ's recent 1.4 and 3.1-GHz profiles are the best quality available, and these show perhaps a central notched core flanked, by a leading conal outrider, and just a hint of the trailing one. Further, the PPA traverse above 1 GHz exhibits a perplexing rotation through more than 180°. Despite these difficulties, the star exhibits what is essentially a core-single profile evolution, and the rough 8.4-GHz detection of JKW may show the surviving pair of conal components. If the vO97 profile provides a reliable sweep rate, then the profile dimensions can be roughly squared with an inner cone geometry as shown in the table.

B1322+83m: Little can be gleaned about this star's emission from the published profiles (GL, KL); however, the high quality GMRT 325-MHz profile in Figure A3 is more scrutible. The star has two regions of emission, one in the form of a highly polarized "precursor" with a completely flat PPA traverse, and then a second region of emission which is also highly linearly polarized but with a positive sweep rate. We take the position that the precursor is unrelated to the polar-cap core/cone emission structures. Then, the "main pulse" is very likely a conal single profile. This configuration would then be very similar to what is observed in the B0943+10 'Q' mode (Backus *et al* 2010). The RVM fit yields α=27°and β=9.2°.

B1356–60: Some published profiles are useless for our purposes because of scattering or poor resolution (vO97, WMLQ, MHQ). However, the two recent polarized profiles (KJ, JKW) suggest a core-single evolution without conal outriders. Interestingly, KJ find a significant, apparently A/R shift, between 1.4 and 3.1 GHz when the profiles are aligned using their SG points (very like what we see for B0540+23 in Fig. 4 above).

B1426–66: Many published observations are available for this southern pulsar (HMAK, MHMA, MHM, MHMb, vO97, J-07, JKW), and most are of good quality. Apart from its odd profile shape, we cannot see why L&M saw this star as a "partial cone". Again, it is the Johnston *et al* (J-05) work that is most insightful. The bright narrow feature marked by antisymmetric V is clearly a core component, and it is flanked by a broad leading component and a weak trailing one. Using the core width to determine α, the conal dimensions and the PA sweep rate, it is clear that an inner cone geometry obtains.

B1449–64: An identical set of observations is available for this prominent southern pulsar (HMAK, MHMA, MHM, MHMb, vO97, J-05, JKW), and while it seems likely that this 180-msec pulsar would generate a core feature, no clear circularly polarized signature is apparent. We do see evidence of conal outriders in both the 1.6 (MHM) and 1.4-GHz (J-05) profiles, and the width of the central (putative) core constrains α to some 43°. A rough estimate of the conal outrider dimension then strongly suggests an inner conal geometry.

B1530+27: It is easy to see why LM placed this pulsar in their "partial cone" category with its bright leading component and weaker, barely resolved trailing one (RSW, BCW, GL, W-99, W-04)—not to mention its weak postcursor. As we see Figure A3, neither its profile nor shallow PPA traverse readily indicate that this could be a conal single or double (**D**) profile. However, the PRAO profiles (MIS, K-98, KL) show that the trailing component becomes as strong as the first at 100 MHz, and HR's time-aligned profiles show how this comes about (properly aligned with a little smaller DM). Moreover both D86 and WES exhibit the star's prominent correlated subpulse motion, showing that the profile is basically conal.

None of this, though, accounts for the star's weak, highly linearly polarized "postcursor" component, which trails its main emission components by some 50°. Please also note that W-04 shows that the PPA traverse under this feature is nearly constant. We could fit the RVM to the main pulse yielding $\alpha = 113°$ and β=9.1°; however the postcursor emission could not be fitted with the same RVM. The "flaring" analysis did not yield any significant sporadic emission at the profile edges. The SG point appears to be coincident with the profile center as measured with respect to the 10% outer widths.

B1530–53 has received no recent study, but indeed it appears to present another good example of the "partial cone" emission envisioned by LM. Just as in the case of B0906–17 above, it shows a bright leading and faint trailing component over a broad frequency band (HMAK, MHMA, MHM, MHMb, vO97), and we see also some evidence for both a "90° jump" on the leading edge and a steep rotation of the PPA across the middle of the profile. The lowest frequency profiles (MHMb) suggest that the trailing component may increase in relative strength at low frequency. Overall, this pulsar's profile seems to represent a very asymmetric conal double (**D**) profile.

B1540–06 exhibits an asymmetric single profile with a steep rise and slow fall-off over a very broad frequency range (MHMb, MGSBT, MIS, GL, KL) as also seen in Figure A4. Its linear polarization is small, especially in the trailing part of the profile, and its PPA behavior disorderly and inconsistent—both frequent properties of conal single ($\mathbf{S}_d$) profiles. It is the WES/WSE work, however, which provides evidence in the form of narrow 0.32-c/P_1 modulation features at both 92 and 21 cms. GL's high frequency profiles suggest a sweep rate of about –14°/°, and the constancy of its profile width over at least four octaves suggests an inner cone geometry.

B1556–44: This is a well studied southern pulsar, and the profile has an asymmetric triple form around 21 cms. with a broad central component and weak conal outriders (WMLQ and MHQ)—probably prompting L&M to see it as a "partial cone". At meter wavelengths its profile has a symmetric single form (LM, MHMA, vO97), and at higher frequencies the central (putative core) component is seen to be composed of two overlapping components (MHQ, J-07). The high frequency PPA traverse shows an orthogonal jump below the conal components. Nonetheless, using L&M's R value and the core width to constrain α, we find that an inner cone $\mathbf{S}_t/\mathbf{T}$ geometry fits very well. We did not find any "flaring" in the PS.

L&M considered the star as an example where the SG point is located towards leading side of the profile, and all the above profiles below 1 GHz show this PPA curvature strongly. Interestingly, the PPA histogram observerd with the GMRT at 325 MHz, shown in Figure A4, does not. The PPA traverse for the central and trailing components is very similar to that at higher frequencies, but shows a non-orthogonal jump (by about 50°) below the leading component. This could result from OPM averaging, and the single pulses are not strong enough to distinguish the modes for the conal components. As a consequence no reasonable RVM fit to the PPA swing was possible. However, based on the average PPA traverse, one can readily see the downward trend from the leading to the trailing edge of the profile.

B1604–00 has been studied extensively and can be observed down to 50 MHz and up to at least 5 GHz (MGSBT, MHMA, MHMb, RSW, GL, HW, vO97, vH, MIS, W-99, KL, K-98). L&M apparently regarded this pulsar has having a "partial cone" profile because of the asymmetric slow rise and steep falloff of its higher frequency profiles—*e.g.*, see Figure A4. We have earlier regarded this pulsar has being a triple (**T**), but its profile does not evolve in the usual manner (*cf.*, HR), and there is no strong indication to the effect that the middle feature is a core component (R88). Its profile evolution is more suggestive of the conal triple class, as the central component's strength diminishes at low frequency and never dominates the profile. Moreover, while the star's PSs exhibit no clear drift, its subpulses seem to show a kind of "moding" and a long period fluctuation feature (WES/WSE). Overall, we can now best regard B1604–00 as having an inner-conal triple (c**T**) profile, such that our sightline at meter wavelengths cuts close to the boundary between its two polarization-modal subcones. It is then likely that the weak leading-edge emission is associated with the outer cone as seen in other pulsars with similar geometries [*e.g.*, B0834+06 and B1919+21 (ET VII)]. As in Paper VI, the values in Table A3 are taken from the mode-separated profiles in R88.

B1612+07 has been observed over a broad band from 0.1 to 5 GHz, and overall it exhibits a barely resolved two-component profile with the leading component consistently brighter; see Figure A4 as well as GL, vH, W-99, W-04, MIS, and KL. It was this consistent asymmetry that probably caused L&M to regard it as a "partial cone". Evidence for subpulse drift comes from D86 and WES/WSE. Moreover, the tendency for the star's low frequency profile to have better resolved components further suggests a conal single ($\mathbf{S}_d$) evolution.

B1641–45: This bright, distant, southern pulsar has been observed repeatedly, but at frequencies below 1 GHz its profiles are corrupted by scattering (MHMA, MHM, MHMb, vO97). Only in the 1.4/3.1-GHz profiles of KJ do we begin to see some profile structure, but the conal outriders are far from clear, and the PPA traverses are impossible to decipher. However, the 8.4-GHz polarized profile recently measured by JKW clarifies matters completely. Here we see that the PPA traverse is essentially central, and the outside dimensions of the outrider pair can be reliably determined. This is the basis of the inner-cone $\mathbf{S}_t$geometry determination in Table A3.

B1648–42: Only two observations (vO97, WMLQ) are available for this wide profiled pulsar, and both show two components with a prominently steepening PPA traverse—indeed, probably it was on this basis that L&M came to regard the pulsar as a "partial cone". Here, we have no basis to decide on whether a trailing portion of the profile is "missing", or whether the profile is complete as it is. In either case a simple geometric model can be assembled to suit the situation: in the first case, probably a c**T** would be invoked, and in the latter situation a conal double (**D**) configuration. Table A3 gives values for the latter case.

B1700–18: In addition to our Figure A5, profiles have been published for this somewhat weak pulsar only by GL and S95. The star's asymmetrical single profile undoubtedly accounts for its "partial cone" status in L&M's effort. The strongest evidence, however, comes from WSE, who find drift-associated modulation with a P_3 of about 3.5 P_1 as well as a strong low frequency modulation feature. The star's profile must then be of the conal single type, and indeed, many such profiles are quite asymmetric. We find some "flaring" in the star's PSs as seen in Fig. A5, and either this pattern or the average profiles can be used to obtain a half-power width of about 12°. Similarly, an RVM fit to the PPA traverse yields α and β values of some 166 and –1.7°, respectively—from which a maximum sweep rate of –8.4°/° can be computed. The SG point lags the center of the outer conal "flared" profile by about 1.7°—apparently due to A/R—giving a very reasonable radio-emission height of 279 km.

B1732–07: Figure A5 gives our 325-MHz GMRT profile, and other published observations are available from GL, vH, J-07, and S95. At meter wavelengths the star's profile is somewhat asymmetric, and perhaps this is why L&M regarded it as a possible "partial cone". In fact, there can now be little doubt but that this star has a triple (**T**) profile with a central core component. WES/WSE find no evidence of conal modulation features, the star's PPA traverse is highly central, and α can be estimated from the core width. Significant "flaring" can be seen in Fig. A5 that appears to coincide with the three profile components. All these circumstances square in the outer conal geometry of Table A3. The midway point of the "flared" profile leads the peak of the central core component by 2.3°. This gives an A/R conal emission height of 205 km with respect to the core (see G&G).

B1742–30: This pulsar's geometry has long presented something of a mystery—and indeed it appears to have been to L&M who listed this star as a possible "partial cone". Several of the older published profiles (MHMA, vO97, XRSS) do not show its full extent, but the long, weak trailing portion is visible in all of LM's observations, that of WMLQ, and the GMRT 325-MHz polarimetry of Figure A5. Nor is it easy to interpret the PPA rotation across the various profiles, but apart from several "90° jumps" and the "hat" above the bright, central component, one can interpret the traverse as basically flat and central. The trailing part of the merged main feature thus appears to be a core, with two components preceeding it and the two trailing components merged in the long "tail"—reminiscent of B1237+25 in its "abnormal" mode. Fig. A5 further shows most of the five components in the "flaring" analysis, and here the core appears independently enough to measure its half-power width. With all this information and interpretation, the double cone/core geometry of the pulsar is assembled quantitatively in Table A3. Our RVM fits to the PPA yield α=177°and β=-4.2°, however the SG point is not well constrained. An A/R height can be estimated for B1742–30's outer cone with respect to its central core feature (see G&G). The outer cone's midway point the core peak by some 1.14°, yielding an emission height of 87 km.

B1745–12: The pulsar has been observed at several frequencies by GL, XRSS and S95. The pulsar's highly asymmetric profile at meter wavelengths surely led L&M to see it as a possible "partial cone"; however, three (or possibly four) components can be discerned at higher frequencies. The GMRT observation at 325 MHz in Figure A5 clearly shows two components as well as a long weak trailing "tail". The PS polarization is weak, but the average shows that the PPA traverse is flat under the leading components (with an OPM "jump") but steepens to an SG point near the middle of the overall profile center. We have fitted the OPM-corrected average PPA traverse to the RVM, and the SG point is the longitude origin in the figure—however this SG point is poorly contrained by the lack of polarized emission in the weak, trailing part of the profile—giving α=167° and β=–1.1°.

A search for "flaring" in the trailing portion of the profile identified 14 occasions as indicated by the green curve in Fig. A5. No evidence for periodic modulation was found in the PSs, and indeed the WES/WSE fluctuation spectra are completely featureless. We cannot then be sure about this star's classification, but the weak speading of its outer conal components appear to reflect an outer cone, and this dimension together with the resultant –11°/° sweep rate provide a basic quantitative geometry in Table A3 which seems compatible with the available observational evidence. Also, the SG point lags the midway point between the outer conal component pair of the "flared" profile by 2.6° giving an A/R emission height for the outer cone of 215 km.

B1756–22: Apart from GL's five polarimetric profiles, only the 1.4-GHz total power observation of S95 has been published; and both spectra of WES/WSE are entirely featureless. The PPA traverse does seem to be nearly flat, and the width of the bright putative core component roughly compatible with an orthogonal magnetic colatitude. Putting this interpretation into Table A3, we find that it is compatible quantitatively with an inner cone/core ($\mathbf{S}_t$) emission geometry.

B1822–09: With both its interpulse and precursor component, (see Figure A6), this pulsar's geometry has been debated actively since near the time of its discovery. A great many published studies are available (MHMA, MHM, SVS, vO97, MGSBT, MHMb, GL, vH, MIS, KL, K-98, X-95, KJ, J-07, WES/WSE), and surely L&M had adequate reason by virtue of its apparent main-pulse asymmetry to view it as a "partial cone". However, we take the position that the precursor and main pulse are separate entities (Backus *et al* 2010), so our geomteric analysis here follows that in this study and applies only to the main pulse. Our PS analyses of it indicate that this structure represents an inner cone/core triple (**T**) profile with a nearly central sightline trajectory. The RVM fit in Figure A6 is for α=166°and β=-0.3°.

B1842+14: Figure A6 gives our 327-MHz Arecibo profile, and many other published observations are available (RSW, vH, GL, HR, MIS, W-99, J-07, WES/WSE). Again, it is not clear what caused L&M to regard this star as a possible "partial cone", but its flat PPA traverse and steep upturn (see W-99 and J-07) might well have suggested that a further trailing component was missing. Perhaps. The core-single evolution and quantitative geometry fits the pulsar rather well (ET VI)—that is, apart from the unusually flat initial PPA, too sharp upturn, and disparity between the two putative conal components above 1 GHz. The delayed upturn might be caused by an A/R shift, but this idea does not seem to fit. One other possibility is that the flat PPA represents emission from a highly polarized precursor, and that the remaining parts of the profile represent a core-single structure. However, without quality higher frequency profiles to draw on, this possibility cannot be evaluated. Therefore, we retain the first model in the table.

B1851–14: For this pulsar we have little to go on apart from the few published profiles (L90, XRSS, GL, WSE) and our GMRT 325-MHz profile in Figure A6. Our "educated" guess is that the profile is of the conal single ($\mathbf{D}_d$) type, and the quantitative geometry in the table is compatible but not well constrained. Some confirmation might come from the fluctuation spectra,but both our own and that of WSE are featureless.

(B1859+07): This pulsar was not among the L&M "partial cone" grouping, but probably would have been included had they known of it. Its asymmetric profile is subject to occasional "events" during which emission in single pulses moves to earlier longitude (see RRW). Otherwise, we found few published references to this pulsar (GL, W-04, WSE), which unfortunately provide little further insight. The quantitative geometry in Table A3 is taken verbatim from RRW.

B1900+05: Again, this pulsar's asymmetric profiles (MGSBT, RSW, GL, W-99, WES/WSE), also Figure A6, probably encouraged L&M to regard it as a possible "partial cone". Beyond this, there is little clear evidence to go on. Both Paper VI and W-99 classified it as a core-single star, but no core signature can be discerned in any of the existing profiles. This classification still seems likely, but the profile width—and thus the geometrical model—in Paper VI are incorrect. We have repaired this error above in Table A3 on the basis of revised estimates.

B1907–03: Here the published studies clearly show a core/cone triple ($\mathbf{S}_t$) profile at 21 cms. (GL, S95), whose core is even marked by sign-changing circular polarization, and a single profile at 408 MHz (L90). Our GMRT 325-MHz profile in Figure A7, unfortunately, is useless owing to its distortion by scattering, and no useful information comes from the fluctuation spectra in WSE. Most observations suggest a flat, central PPA traverse, and this together with the profile dimensions fixes an inner cone/core geometry quantitatively.

B1910+20: The pulsar was classified as a "partial cone" by L&M with the SG point lying towards the trailing edge of the profile. Average profiles at 610 and 1410 MHz (GL) show a strong leading and weak trailing component. These PPA traverses appear complex such that no clear interpretation can be made. However, the 1.4-GHz profiles of W-99, RSW and this paper, Figure A7, show the full PPA behavior in some detail. The latter in particular is complex and cannot be described by the smooth RVM curve, but the expected underlying 'S' shape is evident—although the poor fit precludes determining the SG point with any precision. Our efforts to fit the RVM yields α=171°and β=0.3°.

The available pulse-modulation studies (D86, WES/WSE) leave no doubt that the profile represents a double conal structure: the outer conal components show a fairly regular stationary modulation with a P_3 of about 2.7 P_1, and we see evidence (*e.g.*, DHCR) that this modulation is shared by the inner conal components as well. We have found no evidence of flared emission at the profile edges. Our LRF spectra in Fig. 2 yields signatures of the 2.7-P_1 P_3 modulation in the outer conal component pair.

As no clear signature of a core component can be seen in any profile, its width cannot be determined. We do see hints of core activity including antisymmetric V in some profiles, but overall we cannot resolve whether this profile is of the **M** or c**Q** type. However, using the PPA fit above and the profile dimensions from Paper VI, a slightly revised quantitative model of the emission geometry can be found in Table A3. Although the SG point is not well constrained, our measurements show that the midway point leads the SG point by only 0.5°, giving an emission height of about 228 km.

B1913+10: Little more can be said about this pulsar's geometry than was possible in Paper VI. The 4.85-GHz profile is so poorly resolved that no structure can be seen, and the 400-MHz profiles have scattering "tails". The recent, well measured profiles of J-07, W-99 and Figure A7 resolve a feature on the profile's trailing edge at 1.4 GHz that becomes very pronounced at 3.1 GHz. The one available LRF (WSE) is featureless. It still may be that this is a core-single star, but no geometrical solution bears this out. The two resolved components at 3.1 GHz cannot be interpreted as a conal outrider pair: their outside dimension is much too small for them to be an inner cone.

B1915+13: In slighly poorer observations this pulsar exhibits only a single narrow Gaussian-shaped component, but when resolved optimally it has an unresolved feature on its trailing edge. This structure is clearly seen in the 1.4-GHz profiles of BCW, EW, W-99, HR and Figure A7—and these and many other observation also show an accelerating PPA rotation such that the SG point falls far on the trailing edge of the profile (GL, RSW, RB, vH)—and very like that of B0540+23 above where the shift increases with wavelength.

PPA fits by BCW and EW as well as ourselves at 1.4 GHz consistently show that the SG point falls far on the trailing edge of its profile, and GL's lower frequency profiles suggest even greater displacements, such that A/R effects provide a natural explanation. The star's fluctuation spectra are featureless (WES/WSE), and the weak "flaring" in the above figure does not seem indicative of conal emission. Interestingly, the pulsar has been detected down to 100 MHz (KL, MIS). For all these reasons we classify this star as having an arSt profile. Our RVM fit yields α=101°and β=-5.7°.

B1924+16: This pulsar exhibits a single component with a long slow rise on its leading edge. The published profiles give a mixed impression regarding the curvature of PPA traverse (RB, BCW, RSW, GL, vH, W-99), but the fits by BCW and ourselves in Figure A8 concur in showing a slight upward acceleration and thus placing the SG point toward the trailing edge of the profile (the longitude origin in the above figure). Weak indication of a long (about 60 P_1 modulation) is seen in the fluctuation spectra (WES/WSE), but overall there is little indication of conal activity. On this basis we designate the pulsar as having an arSt profile. The RVM fits to the PPA yield α=5.4 and β=1.4°, respectively. The midway point of the profile calculated using the outer peaks of the "flared" profile leads the SG point by roughly 4.1°, giving an A/R height of about 506 km.

B1930+22: This fast, highly dispersed pulsar is difficult to observe at lower frequencies, and only the 1.4-GHz profiles of GL, BCW, W-99 and the AO observation in Figure A8 fully show its fast rise and slower falloff. Several of the observations suggest an upwardly curved PPA traverse, and our RVM fit (with α=22°and β=4.1°) concurs with that of BCW in placing the SG point about halfway down the trailing side of the profile. The significance of this placement is not yet clear: One might attribute this configuration to A/R as we have several times above; however, the "flaring" on the two edges of the profile suggests some conal activity there—and indeed, the dimensions are compatible quantitatively with the geometry of an inner cone (see Table A3). Possibly A/R does shift some high-altitude core emission earlier so as to overlie the leading conal feature, but new high quality observations are needed at lower frequencies to assess this possibility. We then retain the $\mathbf{S}_t$ designation of Paper VI but amend it to show the probable role of abberation/retardation. Using both the "flared" and the average profiles, the center of the conal peaks lead the SG point by 3.2°. This shift provides an A/R-height estimate of 96 km for the conal emission.

B1937–26 shows a consistently asymmetric profile that prompted L&M to regarding it as a "partial cone" (GL, WMLQ, vO97, vH, MHQ). A bright leading and weak trailing feature are seen in all the star's profiles, but in several of the higher frequency profiles (including the J-05 that is best resolved), we see a suggestion of a third feature on the leading edge. Further, the fluctuation spectra (WES/WSE) suggest conal emission as does the "flaring" in our GMRT 325-MHz observation in Figure A8. We cannot then resolve just how the profile should be classified, but using the fitted PPA sweep rate and conjecturing that the high frequency profile width reflects the core width, the geometry in the table is compatible quantitatively with an inner cone. RVM PPA fitting yields α=171° and β=-2°, but given the shallow PPA traverse the SG is not well constained. Nonetheless, using the "flared" and average profiles the midway point of the profile leads the SG point by 0.8° giving an A/R height estimate of about 70 km.

B1944+17: The pulsar's main-pulse profile (see Figure A8) superficially resembles some of the conal "partial cone" objects we have identified above (*e.g.*, B1540–06) with weak emission on their trailing sides (*cf.*, HR), but the detailed published studies leave little doubt that this star is correctly classed as having a conal triple/quadruple (c**T**/c**Q**/) profile. The pulsar has several modes, some with orderly drift (Deich *et al* 1986; WES/WSE), and these together with its $\gtrsim$60% null pulses make its profiles somewhat unstable (MHMA, MHM, MGSBT, RSW, vO97, vH, W-99, MIS). Its shallow, linear PPA rotation and orderly profile evolution (*e.g.*, HR) further support this understanding of its emission geometry. Indeed, in a recent study by Kloumann & Rankin (2010) the pulsar's geometry has been analyzed in detail; the values in Table A3 are taken from this work.

B1944+22: The two existing AO profiles (RB, W-99) of this weak pulsar reveal only that it has two unresolved components—much as seen in Figure A9—the second of which is much weaker. The profile is almost certainly conal, and thus its behavior is very likely akin to that of the many conal single (or inner-cone double) stars with weak or missing trailing emission. If the W-99 PPA rate is reliable, then we can easily compute a model for the star's geometry as in Table A3.

B2021+51: This bright pulsar has been studied for many years, and most evidence points to its having a conal single ($\mathbf{S}_d$) profile that shows the characteristic low frequency bifurcation with a much weaker leading component (M71, MGSBT, vH, GL, X-95, KL, K-98); see especially K-98. This behavior is thus very similar to that of B0809+74 (*e.g.*, RRS). Both its SVM PPA traverse and subpulse-drift modulation (ETIII; WES/WSE) are also largely compatible with this understanding. Interestingly (and unusually) the pulsar's leading edge emission is fully linearly polarized at metre wavelengths (as is B0809+74's at frequencies above 1 GHz) such that the one active polarization mode here must be completely linearly polarized. Note in Figure A9 that both OPMs are active only under the trailing component. In Table A3 we revise slightly our earlier emission model in Paper VI: surely the pronounced conal speading seen in K-98 argues for an outer-cone geometry, and we use the results of the PPA fit (with α=5.4°and β=1.4°) in the above figure. The "flaring" analysis for this star shows only weak, occasional emission on the profile edges. These do provide a means of estimating the profile's midpoint—which leads the fitted SG point by about 1.1°—giving an A/R emission-height estimate of 113 km.

B2043–04: The published profiles of this pulsar all show a symmetrical single form with a "soft" leading edge (GL, vO97, MIS). It is thus not very clear why L&M regarded it as a possible "partial cone". The 325-MHz GMRT profile in Figure A9 is the only one that it well enough resolved to indicate two features as well perhaps as "flaring" on its leading edge. There can be little doubt that the profile is conal, probably an inner cone $\mathbf{S}_d$ with occasional outer conal subpulses on the far leading edge (as seen in some other such pulsars, *e.g.*, see B1604–00). This understanding is corroborated strongly by WES/WSE's analyses showing a strong narrow fluctuation feature at 0.37 c/P_1 that is clearly indicative of subpulse drift. The SG point can be fixed by an RVM PPA fit as shown in Fig. A9, yielding α and β values of 109 and 2°, respectively. The midpoint of the outer conal peaks of the "flared" profile coincides with the SG point within the measurement errors, suggesting that A/R is not significant in this slow pulsar.

B2053+36: This pulsar's asymmetric single profile seems to have been the reason for L&M's "partial cone" categorization (RSW, GL, W-99). And, indeed, it is also problematic from our perspective. Its flat segmented PPA traverse is unusual and apparently indicative of a central sightline traverse, even if the "jump" is due to an OPM dominance transition as indicated in Figure A9. Entirely conal profiles are rare in pulsars with such a short period, but we see no hint of core action. Moreover, WES/WSE make a claim for subpulse drift without direction! However, they find no consistent behavior at their two frequencies. No consistent geometrical model can be computed from the available information.

B2217+47 exhibits a somewhat asymmetrical profile over a broad band, and this apparently led L&M to see it as a "partial cone" (GL, SVS, MIS). Our GMRT 325-MHz profile in Figure A10 shows a similar form. We see some hint of conal outriders at 21 cm (K-98 and MGSBT)—and these appear to dominate the profile at 4.9 GHz (SRW)—arguing strongly that the star is a member of the core-single ($\mathbf{S}_t$) class. Interestingly, WES/WSE find some evidence for systematicsubpulse motion at 1.4 GHz, but without a fuller study their result is hard to interpret. These results then provide the needed information to construct the quantitative emission model given in Table A3.

B2217+47, however, shows further unorthodox behaviors that need further study. Downs (1979) found that there was a strange truncated-exponential baseline emission that decayed after the pulse, and MGSBT's profiles were not sensitive enough fully confirm or refute it. Moreover, SS find that the star has a postcursor feature was variable in its intensity and position over a few years. Our search however did not show such a feature in our data.

B2224+65m: This pulsar has two well separated Gaussian-shaped components (MGSBT, GL, LM, vH, K-98, KL) as seen in Figure A10. The trailing one, however, has a flat PPA, apparently causing

L&M to see the profile as a "partial cone" with a missing leading component. Indeed, we classified it as having a $T_{1/2}$ profile in Paper VI. Clearly, we must now view the fully linearly polarized trailing component as being a "postcursor" feature, and the much less polarized leading component as a "main pulse" in its own right. The PPA fit (with α=166°and β=-3.8°) in the figure does seem to fit both features well, but their separation is large—some 35°. This said, we can only estimate α from the width of the putative core main pulse. We see no hint of conal outriders, and WES/WSE report featureless fluctuation spectra. We note that vH finds this pulsar similar to B0355+54; however, we see no evidence of the A/R which is prominent in that star's PPA traverse.

B2327–20: As shown in Figure A10 the pulsar has a triple profile with a weak trailing component. This is much clearer in the well resolved GMRT profile than in many of the published ones (MHMA, MHMb, MGSBT, vH, vO97, GL, CMH), especially at high frequency where the weak component can be gleaned only as an inflection on the trailing edge. Only J-07's 691-MHz profile provides comparable clarity. Clearly, this star became one of L&M's best examples of "partial cone" profiles. The remaining question is whether the star has an entirely conal triple profile or a core-cone triple one, and this question is difficult to fully resolve. However, the intensity dependence of the central feature and its aberrant PPA behavior tilts in favor of it being a **T** pulsar. WES/WSE find a 50-P_1 feature shared by both the leading and middle components that could be null-related, whereas the weaker 0.39-c/P_1 modulation seems to be present only in the leading component. Apart from the now much better measured PPA rate, taken from the fit in the figure, the quantitative geometry in Table A3 follows the earlier analysis in Paper VI. Our RVM fit to the PPA traverse yields α=153°and β=0.6°, and the center of the outer conal peaks coincide with the SG point within the measurement errors. This behaviour is consistent with other slow pulsars showing little or no A/R effect.